RIGA TECHNICAL UNIVERSITY

Renārs Millers

SIMULATION MODEL FOR COOLING PANELS WITH INTEGRATED LATENT THERMAL STORAGE SYSTEM

Summary of the Doctoral Thesis

RTU Press
Riga 2021

RIGA TECHNICAL UNIVERSITY
Faculty of Civil Engineering
Institute of Heat, Gas and Water Technology

Renārs Millers
Doctoral Student of the Study Programme "Heat, Gas and Water Technology"

SIMULATION MODEL FOR COOLING PANELS WITH INTEGRATED LATENT THERMAL STORAGE SYSTEM

Summary of the Doctoral Thesis

Scientific Supervisor
Professor Dr. sc. ing.
ARTURS LEŠINSKIS

RTU Press
Riga 2021

Millers, R. Simulation Model for Cooling Panels with Integrated Latent Thermal Storage System. Summary of the Doctoral Thesis. Riga: RTU Press, 2021. 46 p.

Published in accordance with the decision of the Promotion Council "RTU P-12" of 23 February 2021, Minutes No. 1/21.

https://doi.org/10.7250/9789934226281
ISBN 978-9934-22-628-1 (pdf)

DOCTORAL THESIS PROPOSED TO RIGA TECHNICAL UNIVERSITY FOR THE PROMOTION TO THE SCIENTIFIC DEGREE OF DOCTOR OF SCIENCE

To be granted the scientific degree of Doctor of Science (Ph. D.), the present Doctoral Thesis has been submitted for the defence at the open meeting of RTU Promotion Council on 3 September 2021 at 15.00 at the Faculty of Civil Engineering of Riga Technical University, 6B Kipsalas Street, Room 106.

OFFICIAL REVIEWERS

Associate Professor Dr. sc. ing. Jurģis Zemītis
Riga Technical University, Latvia

Associate Professor Dr. sc.ing. Sandra Gusta
Latvia University of Life Sciences and Technology, Latvia

Professor Dr. sc. ing. Martin Thalfeldt
Tallinn University of Technology, Estonia

DECLARATION OF ACADEMIC INTEGRITY

I hereby declare that the Doctoral Thesis submitted for the review to Riga Technical University for the promotion to the scientific degree of Doctor of Science (Ph. D.) is my own. I confirm that this Doctoral Thesis had not been submitted to any other university for the promotion to a scientific degree.

Renārs Millers ……. (signature)

Date: ……

The Doctoral Thesis has been written in English. It consists of an Introduction; 7 Chapters; Conclusions; 47 figures; 17 tables; the total number of pages is 105. The Bibliography contains 162 titles.

CONTENTS

ABBREVIATIONS

CFD	Computational fluid dynamics
PCM	Phase change materials
ODP	Ozone depleting potential
GWP	Global warming potential
HVAC	Heating, ventilation and air-conditioning
EPBD	Energy performance of buildings directive
NZEB	Nearly zero-energy building
RES	Renewable energy source
TABS	Thermally active building structure
MEP	Mechanical, electrical and plumbing systems
EER	Energy efficiency ratio
DEC	Direct evaporative cooling
EATHE	Earth to air heat exchanger
COP	Coefficient of performance
SCOP	Seasonal coefficient of performance
TES	Thermal energy storage system
NMF	Neutral model format
IDA ICE	IDA Indoor Climate and Energy
RMSE	Root mean square error
3D	Three-dimensional
ZEB	Zero-energy building

1. INTRODUCTION

1.1. Novelty and Motivation

For the last decades the need for cooling of indoor premises has increased in Central European as well as Northern European climate.

According to the estimations this trend will continue. It is reflected by the fact that the worldwide final energy consumption for cooling has more than tripled in the time period from 1990 to 2016, and according to estimations the energy consumed by cooling equipment will triple again by year 2050 [1]. Particularly large increases in cooling energy growth have been observed in the residential sector.

Currently mechanical cooling is responsible for approximately 20 % of total energy consumption in buildings in Europe [1].

It is clear that the increase of cooling demand is in conflict with the EU movement towards reducing greenhouse gas emissions. New passive cooling technologies are essential to address overheating issues and avoid the increase of installation of cooling equipment that contains refrigerants with high ODP and GWP potentials.

It is known that in most cases passive cooling technologies are not sufficient to cover all cooling requirements in a building. This issue at least partly can be addressed by incorporating thermal energy storage systems.

The main focus of the research is set on the development of a validated equation based simulation model for a ceiling based cooling panels with integrated latent thermal storage system for a previously developed cooling panel.

The development and validation of such simulation model is necessary to accurately predict the behaviour of these panels in modern NZEB buildings using dynamic energy simulation tools preparing this system to be industry-ready.

Validated numerical based simulation models for this type of cooling panel with integrated thermal storage system that utilises bulk PCM have not been developed before and, therefore, can be considered novel.

1.2. Aim and Scope

This thesis aims to develop a calibrated simulation model of a cooling panel with integrated PCM storage and test its applicability for adaptation in full scale building simulation models. The simulation model was developed in *IDA Indoor climate and energy* software. The hydronic cooling panel with integrated PCM storage was developed in the scope of a previous *European Regional Development Fund* research project *No.1.1.1.1/16/A/007 "A New Concept for Sustainable and Nearly Zero-Energy Buildings."*

This Thesis attempts to demonstrate that it is possible to reach a reasonable accuracy reproducing measurements from a physical experiment in a test chamber and a more sophisticated CFD simulation model using a simulation model developed in *IDA ICE*.

This approach was chosen because despite the fact that CFD simulation methods are the most accurate mathematical representations of physical processes their applicability for practical heating/cooling load calculations as well as whole year energy calculations in buildings is very limited. The use of CFD simulations for this purpose is impractical due to labour intensity and very significant computing power required. Nevertheless, dynamic simulation tools allow simulating large systems in relatively small time periods and such simulation tools are widely used in the industry.

Hypothesis

Experimentally validated equation based numerical simulation model of a hydronic cooling panel with integrated latent thermal storage can produce simulation results with accuracy suitable for application in construction industry to support other passive cooling technologies.

1.3. Thesis Task

To achieve the aim of the Thesis several tasks are laid out.

- To perform a state of art literature review for:
  - NZEB requirements in different EU member states;
  - previous studies regarding passive cooling technologies;
  - different PCM materials and their properties;
  - different latent thermal storage applications in buildings and existing numerical models;
  - fundamentals of heat transfer in HVAC systems.
- To describe the methodology, experimental set-up and numerical models used for the study.
- To perform experiments and gather data.
- To perform calibration and validation of the elaborated model against experimental results and results acquired from a CFD simulation.
- To analyse the results in context of other similar studies.

1.4. Thesis Practical Value

Without a reliable thermal storage it is difficult for the majority of currently existing passive cooling technologies to provide sufficient cooling in buildings. This results in increased energy consumption and lowered thermal comfort levels in new buildings. The developed equation based numerical model can be applied by industry professionals for practical whole building scale simulations for HVAC system sizing, thermal comfort and annual energy simulations without using complex and time consuming CFD simulation tools.

The key results of this Thesis and the developed equation based simulation model have been published in open access journal *Energies* by *Multidisciplinary Digital Publishing Institute* [2].

1.5. Arguments for the Defence of the Thesis

- The experimental results demonstrate a reasonable agreement between the measured and simulated results.
- Results produced by the developed model demonstrate a reasonable agreement with the results produced by CFD simulation in a comparative study. The time required for the same simulation case is several orders of magnitude smaller.
- The accuracy of the results produced by the simulation model are equal or more accurate than reported in other similar studies.

1.6. List of Conferences

26.05.2019.–29.05.2019.
Renars Millers, Aleksandrs Korjakins, Arturs Lesinskis. Thermally Activated Concrete Slabs with Integrated PCM Materials CLIMA 2019, Romania, Bucharest.

05.10.2016.–07.10.2016.
Renars Millers, Uldis Pelite. Survey of Control Characteristics of Circular Air Dampers in Variable Air Volume Ventilation Systems, SBE16 Tallinn and Helsinki Conference; Build Green and Renovate Deep, Estonia, Tallinn.

22.05.2016.–25.05.2016.
Galina Stankevica, Andris Kreslins, Anatolijs Borodinecs, Renars Millers. Achieving Deep Energy Retrofit in Latvian Public Building – Simulation Study CLIMA 2016, Denmark, Aalborg.

1.7. List of Publications

Paper 1

Millers, R.; Korjakins, A.; Lešinskis, A.; Borodinecs, A. Cooling Panel with Integrated PCM Layer: A Verified Simulation Study. Energies 2020, doi:10.3390/en13215715.

Paper 2

Millers, R., Korjakins, A., Lešinskis, A. Thermally Activated Concrete Slabs with Integrated PCM Materials. No: *E3S Web of Conferences*, Romania, Bucharest, 26–29 May 2019. Bucharest: CLIMA 2019 Congress, 2019, pp. 1–6. ISSN 2555-0403. Available: doi:10.1051/e3sconf/201911101080

Paper 3

Prozuments, A., Vanags, I., Borodiņecs, A., Millers, R., Tumanova, K. A Study of the Passive Cooling Potential in Simulated Building in Latvian Climate Conditions. From: *IOP Conference Series: Materials Science and Engineering*, Latvia, Riga, 27–29 September 2018. UK: IOP Publishing, 2017, pp. 1–8. ISSN 1757-8981. Available: doi:10.1088/1757-899X/251/1/012052

Paper 4

Ovchinnikov, P., Borodiņecs, A., Millers, R. Utilization Potential of Low Temperature Hydronic Space Heating Systems in Russia. *Journal of Building Engineering*, 2017, Vol.13, pp. 1–10. ISSN 2352-7102. Available: doi:10.1016/j.jobe.2017.07.003

Paper 5

Stankeviča, G., Krēsliņš, A., Borodiņecs, A., Millers, R. Achieving Deep Energy Retrofit in Latvian Public Building – Simulation Study. From: CLIMA 2016: Proceedings of the 12th REHVA World Congress. Vol.10, Denmark, Aalborg, 22–25 May 2016. Aalborg: Aalborg University, Department of Civil Engineering, 2016, pp. 1–9. e-ISBN 87-91606-35-7.

Paper 6

Millers, R., Pelīte, U. Survey of Control Characteristics of Circular Air Dampers in Variable Air Volume Ventilation Systems. Energy Procedia, 2016, Vol. 96, pp. 294–300. ISSN 1876-6102. Available: doi:10.1016/j.egypro.2016.09.152

1.8. Thesis Composition and Outline

This Thesis is comprises nine chapters.

- Chapter 1 presents the motivation and novelty of the research, defines the aim and scope of the Thesis, formulates the hypothesis, describes the tasks and demonstrates the practical value. Additionally, publications and participation in conferences are listed in this chapter.
- Chapter 2 outlines underlying principles of nearly zero-energy buildings (NZEBs) and examples of the requirements for different EU member states and how overheating issues are addressed in these countries.
- Chapter 3 describes previous research of passive cooling technologies that can be considered as candidates for application in NZEB buildings together with latent thermal storage systems in order to address overheating.
- Chapter 4 includes a review of available PCM materials, their properties and suitability for application in PCM cooling panels. Moreover, this chapter acknowledges property decay over time for different PCMs;

- Chapter 5 describes previous research of latent thermal storage systems and reported performance for different types of TES systems, previously developed numerical models and highlights the most visible experimental and simulation studies.
- Chapter 6 outlines the fundamentals behind heat transfer in HVAC systems in relation to cooling panels that is important to understand to apply, develop and model TES system components.
- Chapter 7 presents experimental methods used in the study and describes the equation based numerical model of the cooling panel with integrated latent thermal storage systems.
- Chapter 8 presents validation of the developed simulation model against experimentally measured values and previous CFD study as well as statistical analyses. Moreover, this chapter describes the limitations of the developed numerical model.
- Chapter 9 summarizes the conclusions of the work done and confirms the hypothesis.

2. REVIEW OF NEARLY ZERO-ENERGY BUILDING REQUIREMENTS IN EUROPEAN UNION

EU aims to limit CO_2 emissions in building sector by 55 % (compared to 1990 levels) by year 2030 and reach net zero greenhouse gas emissions by year 2050 [3]. Currently building segment contributes to around 40 % of total CO_2 emissions in EU and represents the largest source of emissions in Europe [4].

The main tool for reducing energy consumption in buildings and reaching net zero greenhouse emissions by 2050 in EU is the Directive 2010/31/EU of the European Parliament and of the Council on the energy performance of buildings. This directive states that by 2020 December 31 all new buildings must be "nearly zero-energy buildings".

The directive provides only general framework for the calculation methodology of NZEBs as well as minimum energy requirements for NZEBs – these details are to be described in the building codes of all the member states and shall be cost-optimal.

Heating energy consumption can be significant especially in the northern and central part of Europe, and this has been extensively addressed in the past decades. Many countries have adopted requirements in building codes that result in highly insulated, airtight buildings to minimize heating energy consumption. Ovchinnikov et al. [5] also have emphasized the benefits of low temperature hydronic heating.

For northern and central part of Europe where NZEB and low energy buildings are usually airtight with highly insulated envelopes the accumulated internal and solar heat gains can be trapped within the thermal envelope that can lead to increased overheating in rooms.

This overheating side-effect of modern northern European buildings must be addressed in the building codes and handled in efficient manner. Many countries have already incorporated some type of limitations for maximum indoor temperatures.

Austria had building codes with relatively well-defined energy performance requirements for new buildings and major renovations already before the Energy Performance Buildings Directive (EPBD) came into power. This can be partly contributed to the "Passive house" movement before the introduction of the NZEB concept.

NZEB in Austria is defined as an energy efficient building with good thermally insulated envelope and an environment-friendly heating system. Energy performance is measured by four indicators:

- space heating demand (kWh/m^2 a year);
- primary energy demand (kWh/m^2 a year);
- CO_2 emissions (kg/m² a year);
- total energy efficiency factor.

Compliance to NZEB performance can be demonstrated in two ways:

- through meeting the space heating demand requirement;
- through meeting the total energy efficiency factor.

For both cases also maximum primary energy consumption and CO_2 emissions are limited. For space heating demand calculation also building shape factor is considered.

Overheating in residential buildings in Austria is addressed as a limitation of maximum operative temperature of 25 °C and 27 °C depending on the room type and time of the day.

NZEB requirements in **Denmark** are primarily set by limiting primary energy consumption, however, other factors such as overheating, envelope heat transmittance, building air tightness and the use of RES are also limited.

Maximum primary energy consumption in new buildings has been tightened in 2010, 2015 and 2020. Each time by approximately 25 % arriving to NZEB levels in 2020. The NZEB requirements for primary energy consumption are 20 kWh/m² a year for residential buildings and 25 kWh/m² a year for non-residential buildings. This primary energy consumption limit is independent from the size of the building.

Additionally to primary energy consumption, the design transmission loss through building envelope is also limited and must not exceed 3.7 W/m² for single-storey buildings, 4.7 W/m² for two-storey buildings and 5.7 W/m² for three and more storey buildings.

Apart from the energy consumption it also must be demonstrated (using dynamic simulation software or "*Be10*" (a national calculation tool [6])) that the indoor temperature in residential buildings does not exceed 26 °C for more than 100 hours and 27 °C for more than 25 hours a year. If the indoor temperature exceeds these values, an overheating penalty is calculated as an imaginary cooling system that maintains 26 ºC inside the rooms [7].

NZEB requirements in **Estonia** are set by limiting primary energy consumption in buildings. There are separate requirements for different building types.

There are no minimum requirements for *U*-values the building has to meet in order to comply with NZEB requirements.

Apart from energy consumption a limit for overheating in summer (from 1 June to 31 August) is also set to a maximum of 150 degree-hours over 27 ºC for residential buildings and 25 ºC for non-residential [8].

Compliance to the aforementioned primary energy consumption and thermal comfort in summer period must be demonstrated using dynamic simulation software. Energy consumption for residential buildings can also be calculated using a monthly method.

In addition to primary energy consumption there are also mandatory energy efficiency levels for MEP systems.

In **Latvian** building codes until 2015 energy efficiency in buildings was regulated mainly by limiting maximum envelope heat transmission (*U*-values). From 2015 onwards additionally maximum heating energy consumption was introduced.

NZEB requirements in Latvia are set by heating energy requirement, primary energy consumption, minimum ventilation heat recovery, and mandatory use of RES [9].

Apart from energy consumption there is also a limit for maximum *U*-values for different structures and building air tightness [10].

There is no direct requirement for maximum indoor temperatures, however, there is a requirement that during the design stage the client must be informed if indoor air temperature can exceed 28 ºC. However, there is no further information how this must be calculated and how the compliance must be demonstrated [11].

Most countries in the EU have also acknowledged the current issue of overheating in modern buildings and incorporated some kind of measures to address this problem. In most cases there is a limitation of maximum temperature in rooms, defined as maximum temperature or a maximum degree-hour threshold above some room temperature.

It can be concluded that in most of the central and northern EU countries airtight and highly insulated envelopes are required to meet energy requirement demands, but on the other hand this increases the overheating in buildings that needs to be addressed without compromising the overall energy consumption of the building.

3. REVIEW OF PASSIVE COOLING TECHNOLOGIES FOR APPLICATION IN BUILDINGS

From the Chapter 2 it can be concluded that extensive use of passive cooling technologies in buildings is essential for reaching NZEB or even net-zero energy consumption levels in buildings. Many technologies have been previously described in literature but have not yet seen large-scale application in buildings due to high cost, complexity, technical limitations and other factors.

Passive cooling technologies described in this chapter are seen as potential cooling energy sources that can be coupled with PCM storage to address overheating issues and minimize cooling energy requirements in NZEBs, ZEBs.

Night cooling is a passive or semi-passive cooling technique that relies on temperature swings during day and night. The basic concept is to increase the air change in the building during night to utilise the cooler air as a heat-sink.

Night cooling usually is used as a supplement to mechanical cooling to reduce energy consumption or in many cases is coupled with or assisted by other strategies like phase change materials [12]–[15].

Givoni [16]–[18] has suggested that night-time ventilation is feasible in climatic zones where day-time air temperature is below 36 °C and night time temperature is below 20 °C. Roaf et al. [19] found similar criteria: a minimum night-time temperature of 20 °C and maximum day-time temperature of 31 °C.

Artman et al. [20] elaborated a map of Europe based on Meteonorm data [21] with mean daily minimum temperatures and mean differences between minimum and maximum temperatures in July for estimating the feasibility for night cooling in different regions in Europe. Most of Northern and Central Europe is suitable for this cooling technique.

Prozuments et al. [22] performed a simulation study for night cooling potential in Latvian climate. The team found that it is not possible to provide comfortable indoor temperature using exclusively night cooling, however night cooling can provide approximately 8 % energy saving.

Radiant nocturnal cooling is a cooling technique that utilises radiant heat exchange with the sky as a heat sink during the night. The heat exchange takes place because the night sky is cooler than the surfaces on the Earth.

Meir et al. reported that it is possible to cover a significant fraction of a single-family house cooling requirements with radiative cooling system [23]. Ecker and Dalibard [24] found that photovoltaic-thermal collectors can deliver up to 120 W/m² of radiative cooling, and similar values were reported also by Thibault et al. [25].

The importance and potential of the **daytime radiative cooling** using the atmospheric window in the infra-red spectrum between 8 μm and 13 μm was emphasised already a few decades ago [26]–[28]. Only recently daytime radiative cooling significantly below ambient temperatures was demonstrated due to advances in nanophotonics. The key to these advances is the ability for a material to possess a combination of high solar reflectance and strong infra-red emission between 8 μm and 13 μm (Fig. 3.1).

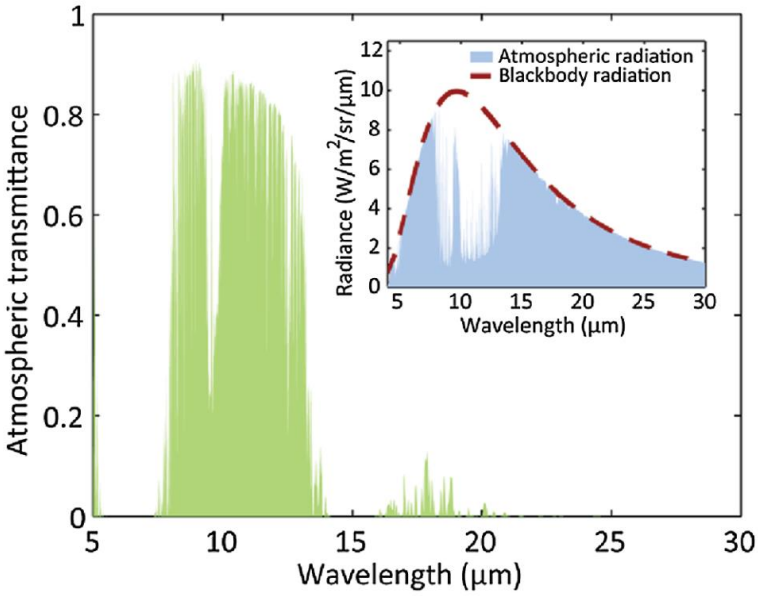

Fig. 3.1. Atmospheric transmittance with downward atmospheric radiation (Figure from [29], data from [30]).

Material with the previously mentioned properties can achieve net positive radiant cooling power even when exposed to solar radiation. This has sparked extensive research in this field after Raman et al. [31] for the first time demonstrated radiant cooling of 5 °C below ambient temperature with the capacity of 40 W/m² under direct sunlight in 2014. Since then, radiant cooling capacities of more than 100 W/m² have been achieved utilising "the window of transparency" in the Earth's atmosphere.

A very common passive cooling technology is **adiabatic or evaporative cooling.** The principle of adiabatic or evaporative cooling relies on the latent phase change energy of evaporating water. The cooling energy is extracted from the process with faster moving water molecules that have enough energy to escape the Knudsen layer or evaporative layer and the rest of the molecules are left with lower kinetic energy. Since the average kinetic energy of the molecules is proportional to temperature the liquid cools. This technology is typically not sufficient to provide enough cooling power all year round, thus it is usually supplemented with other technologies.

Millers et al. [32] in a simulation study demonstrated that it is possible to maintain comfortable indoor temperature in the Baltic Sea region if adiabatic cooling is combined with PCM thermal storage. Duan et al. [33] reported EER values of 30 to 80 for indirect adiabatic cooling equipment. Amer [34] found that evaporative roof cooling was the most effective of the researched passive cooling techniques for arid areas.

Desiccant cooling process consists of dehumidifying an air stream by running it through a desiccant that absorbs or adsorbs the water vapour of the air stream. In a parallel process the same desiccant from a previous cycle is being regenerated by heating it with another airstream to its regeneration temperature that is specific to each desiccant.

After the incoming airstream is being dehumidified, it must be cooled to pre-dehumidification temperature (a common approach is to use air to air heat recovery device). Then the air stream can be cooled with a cooling coil or evaporative humidifier.

Desiccant cooling systems can be feasible if there is waste heat available with sufficient temperature, or alternatively solar thermal energy can be used.

Mavroudaki et al. [35] carried out a simulation based feasibility study for a desiccant cooling system for seven European cities. In the study it was assumed that the cooling system is driven by a combination of a gas boiler and solar collectors. The team found that the moisture content of outdoor air influences the desiccant cooling system more than the availability of solar energy. Solar energy covered from 25 % of heating energy requirements in London to 93 % of heating energy requirements in Oslo.

It is well known that at natural thermal equilibrium conditions the ground temperature at around 3 m depth can be considered constant and is equal to the mean temperature on its surface. This principle is utilized by **passive geothermal cooling**.

Geothermal cooling technologies can be divided in two main categories: **earth to air heat exchangers (EATHE)** and **earth to liquid heat exchangers**. Both technologies are fairly common and extensively researched in the past.

Earth to air heat exchangers have been extensively used and studied. The performance of an EATHE system is related to heat exchange surface (the length and diameter), the air flow rate and other characteristics such as depth, outdoor air conditions and soil properties [36]–[38].

For moderate climates the seasonal passive cooling capacity for most systems is around 8–10 kWh/m² ground heat exchange area a year and peak cooling capacity for 32 °C outdoor air temperature is around 45 W/m² of heat exchange area [39], [40]. Different case studies have reported various performance of the system:

- 20–30 % decrease in discomfort hours in Belgium [41];
- energy savings of 13.1 to 23.8 kWh/m² per year in Germany [42];
- coverage of 1/3 of cooling requirements in Switzerland [39];
- 33 kWh/m² of cooling energy savings a year for a building in Greece [43].

Earth to liquid heat exchanger typically consists of horizontal hydronic circuits or hydronic circuits located inside concrete pile (energy piles) or boreholes. These heat exchangers are usually used for both heat source (using geothermal heat pumps) and as a heat sink for passive and/or vapour compression driven cooling.

For effective use of earth to liquid heat exchangers they shall be utilized for both cooling and heating or regenerated using solar energy or other methods [44], [45]; however, there have been reports that such application leads to a higher failure probability [46].

Most passive cooling technologies cannot cover 100 % of building cooling requirements and have some limitations. Night cooling is highly dependent on outdoor temperature, radiant cooling is dependent on the sky cloud cover, adiabatic cooling as well as desiccant cooling lose efficiency during periods of high outdoor humidity, and geothermal cooling must have annual energy balance, otherwise cooling and heating potential of the ground can be depleted.

It is clear that to fully cover or at least extend the fraction of passive cooling in a building a combination of passive cooling technologies and a suitable thermal energy storage must be used. This is further discussed in Chapters 4 and 5.

4. REWIEV OF PHASE CHANGE MATERIALS

Latent thermal storage systems in principle consist of two components – latent thermal storage medium and heat exchanger in case of active application or a method where and how it is incorporated in the case of passive application. Therefore, the research in PCM field can be divided into two categories [47]:

- material research that deals with development of the PCM itself;
- development of heat exchangers.

The development of heat exchangers is perceived as methods for delivering or extracting the thermal energy from PCMs for different application. This Thesis is mainly concentrated on the energy delivery/extraction methods; however, it is essential to understand the characteristics of PCMs available and the fundamental principles of these materials. This chapter focuses on the PCM itself. The heat exchange methods of energy delivery/extraction from the latent thermal storage are described in Chapter 5.

First studies employing PCM for heating and cooling applications were conducted almost five decades ago by Telkes [48] and Barkmann and Wessling [49]. Since then, this technology has been researched extensively and new commercial and non-commercial materials have been developed.

PCM technologies rarely possess the ability to provide desired thermal comfort in buildings on their own. Thus, generally they are used in combination with other passive (evaporative cooling, nocturnal cooling, night cooling) or non-passive cooling technologies such as vapour compression cooling. PCM in combination with passive technologies are recognized as attractive solutions for passive houses, NZEBs, net zero-energy buildings or even carbon negative buildings. PCM technologies in combination with more traditional cooling equipment are usually used for increasing energy efficiency, down-sizing equipment by cooling power peak-shaving or utilizing lower energy prices during off-peak hours.

PCM is an effective thermal energy storage due to its ability to store energy not only due to temperature change (sensible thermal energy storage) but also due to melting and solidifying (latent thermal energy storage) that takes place at a narrow temperature range. This principle allows storing 5 to 14 times more thermal energy than sensible thermal storage with the same weight and volume.

In 1983, Abhat [50] classified materials that can be used for thermal energy storage (Fig. 4.1). As described in the classification, latent or phase change thermal storage can utilise phase change of gas-liquid, solid-gas, solid-liquid and solid-solid.

A solid-solid PCM [51] utilises the phase change in solid from crystalline to another form. These materials are an alternative option that does not require encapsulation, since it is a solid. Also, these materials have small volumetric changes during phase transition. Clearly these benefits come with a disadvantage of lower latent heat [52]. A good example of solid-solid phase change material is pentaerythritol, pentaglycerine and neopentyl glycol [53].

Another form of PCMs are solid-gas and liquid-gas; physically these materials have the highest latent heat storage capacity, but their practical application is very limited due to

technical limitations. These materials require large volumes making their application impractical. One of few feasible examples is steam accumulators.

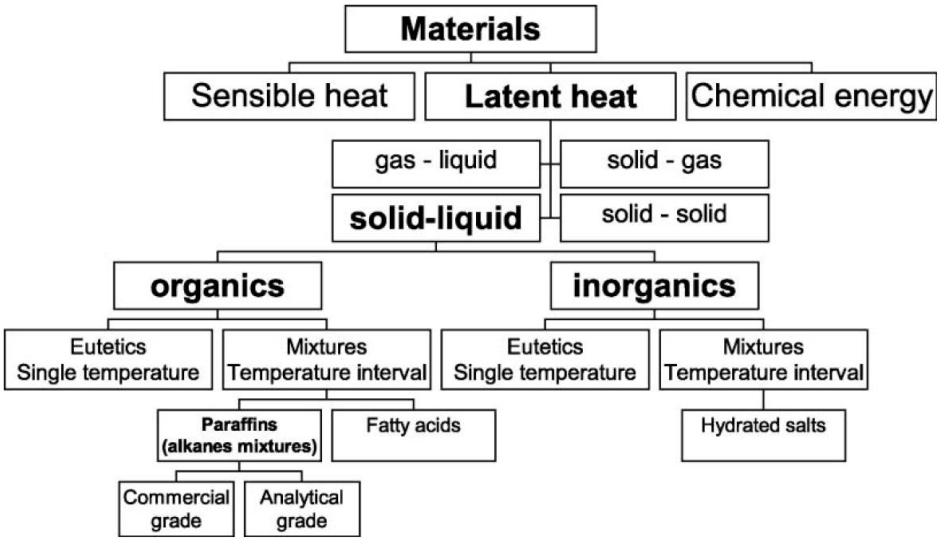

Fig. 4.1. Classification of energy storage materials (information from [50], figure from [47]).

Solid-liquid PCMs have smaller latent energy storage potential if compared with solid-gas or liquid-gas PCMs, nevertheless other favourable characteristics such as small volume change during phase change makes them more feasible and common for thermal storage application. This type of PCM is the most studied, commercially produced and industry ready.

In 1983, Abhat [50] conducted a major study in the field of latent thermal storage substances and produced a classification tree of PCM materials according to their chemical composition. According to Abath [50], there are three main categories of PCMs: organic compounds, inorganic compounds and eutectics.

Another classification of PCMs according to phase-change enthalpy and melting temperatures was provided by Dieckmann and Heinrich [54] (Fig. 4.2).

Most common organic PCMs include fatty acids and paraffins. Paraffins generally have more attractive characteristics that make them more suitable for practical applications. The main advantages of paraffin based PCMs according to Whiffen and Riffat [55] are:

- wide and variable melting point range;
- relatively high heat of fusion (around 120–200 kJ/kg for most materials);
- no super-cooling;
- chemically stable and recyclable;
- good compatibility with other materials (for mixtures) that allows to adjust their melting range.

However, there are also a few disadvantages, for example, their low thermal conductivity [~0.2 W/(m·K)], high volume change during phase transition and flammability.

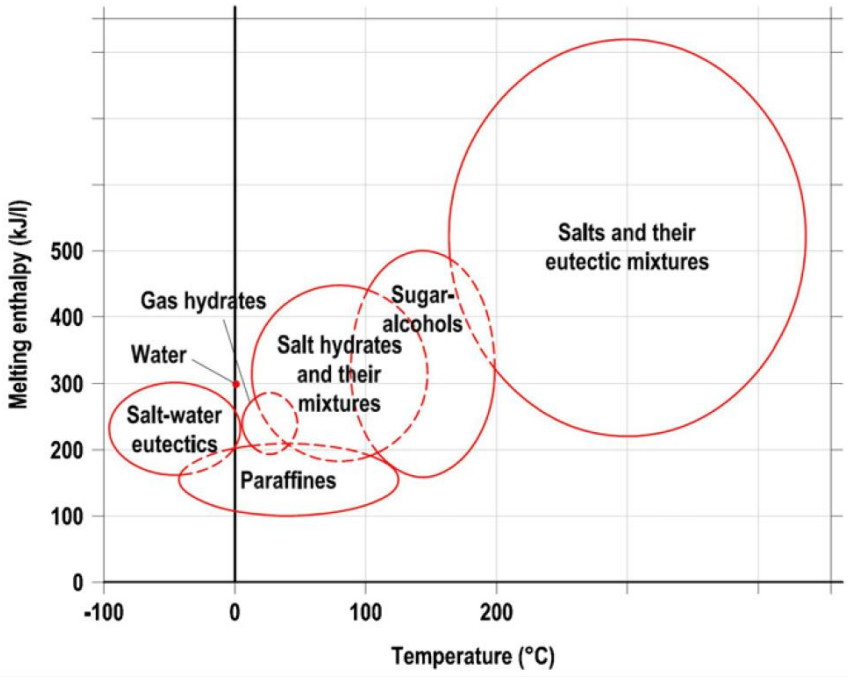

Fig. 4.2. Temperature and latent enthalpy ranges for different types of solid-liquid PCMs.

The thermal conductivity can be enhanced by introducing additional heat conducting mechanisms like aluminium fins [56], carbon micro-fibres [57] or incorporating paraffins in composite materials like paraffin / expanded graphite composite [58]. The flammability of paraffins can be overcome with addition of fire-retardants [59].

Other positive commercially available paraffin properties, pointed out by Beatens et al. [60], include non-corrosivity, non-toxicity, the fact that they do not undergo phase segregation.

According to Beatens et al. [60], the most popular non-paraffin organic PCMs are fatty acids or palmitoleic acids ($CH_3(CH_2)_nCOOH$). These substances have high latent phase-change heat, small volumetric changes during phase transition and narrow range of phase change temperature. The most common fatty acids can be divided into six categories: caprylic, capric, lauric, myristic, palmitic and stearic. The carbon atom count per molecule in these substances range from 8 to 18. The melting-freezing temperatures range from 16 to 65 °C, heat of fusion is between 155 kJ/kg and 180 kJ/kg. However, the cost of fatty acid based PCMs is approximately three times higher than paraffin based. One drawback for fatty acid based PCMs is that there are not many materials with phase transition around 21 °C that can be utilized in passive cooling systems.

Inorganic PCMs generally include salt hydrates, metallic alloys and molten salts, yet the most common inorganic PCMs are hydrated salts. These substances have relatively good thermal conductivity of around 0.5 W/(m·K) (more than two times higher than paraffins), high energy storage density of around 240 kJ/kg. Most of inorganic PCMs are corrosive to many metals and they undergo super-cooling. Hydrated salts are generally significantly cheaper than paraffin based PCMs but slightly toxic.

These PCMs take the form of inorganic salt and water mixtures creating a crystalline solid of general formula $A \cdot nH_2O$, where A represents the salt component. Phase change temperature can be adjusted by varying the chemical composition of salts. The solid-liquid phase transition of salt hydrate is hydration or dehydration of a salt. During melting the hydrate salt either melts to salt hydrate and fewer molecules of water or to anhydrous salt and water [51].

Molten salts have high heat of fusion but also high melting temperature, thus they can be utilized for solar energy storage.

Eutectic PCMs usually are a mixture of two or more substances that solidify and melt congruently. An advantage of these PCMs is that their phase change range is very sharp and can be easily manipulated by changing the ratio of substances in the mixture. However, there is a lack of data regarding the thermal properties of these mixtures.

Previous research in the field of PCMs indicates that fatty acid, and paraffin based PCMs can be utilized to support passive cooling technologies. Paraffin based PCMs have a good combination of cost and performance, and many commercial products are available with a wide range of melting temperatures. These properties make paraffin based PCMs the best candidate for passive cooling applications in the scope of this Thesis.

The next chapter focuses on the energy delivery/extraction methods for the PCM thermal storage. All of the described methods utilise different forms of paraffin based PCMs.

5. REVIEW OF THERMAL STORAGE SYSTEMS BASED ON PCM APPLICATION

This chapter focuses on the previous research in thermal storage systems. PCM thermal storage technologies can in principle be categorized into two categories: passive thermal storage systems and active thermal storage systems.

Passive thermal storage systems mainly rely on incorporation of PCM materials into building structures where they function as a "thermal mass" which stabilizes indoor temperature.

Active thermal storage systems usually employ some mechanical/controlled means of supplying or extracting energy from PCM storage.

5.1. Passive PCM Thermal Storage Systems

The simplest form for integrating PCM into building structures is to mix encapsulated PCM into structural materials such as plasterboards, concrete, etc. or immerse these structures into liquid PCM for the PCM to infiltrate into the pores of the material. This is a very simple form of PCM integration that requires little additional expenses. This method is not very efficient: however, some energy savings can be gained. Hunger et al. [61] reported a 12 % of energy savings by mixing 5 % of microencapsulated PCM into concrete.

The main advantage of passive TES is the lower cost and no energy transportation system required. In this case the PCM is recharged by using night ventilation; however, in most cases this approach does not reach the full potential of the thermal storage. Due to limited area of contact and limited heat transfer coefficients the PCM fails to solidify [62]–[64]. However, there are also examples with impressive energy savings [13], [65].

Integration of PCM into plasterboards is very common, and many numerical and experimental studies evaluating the effectiveness have been conducted [66]–[69]. Kuznik et al. [66] performed a study to test PCM wallboard developed by Dupont de Nemours Society (Fig. 5.1). The wallboard panel was composed of 60 % microencapsulated paraffin with melting temperature of around 22 °C, and the density of the material was 1019 kg/m³.

As a result of numerical modelling the team concluded that the optimum thickness of the wallboard is around 10 mm that represents energy storage of the room for a daily temperature swing from 18 °C to 26 °C for a 24-hour period. The use of the 10 mm wallboard allowed doubling the thermal inertia of the room.

Another team, Berzin et al., conducted a study with PCM wallboards for heating application [65] and night cooling application [13]. The study was performed experimentally with test cabins.

For heating application, the team used an energy price based control system in a combination with floor heating and gypsum board with paraffin based PCM encapsulated in the material. The results indicated 18.8 % energy savings and up to 28.7 % cost savings over a five-day measurement period.

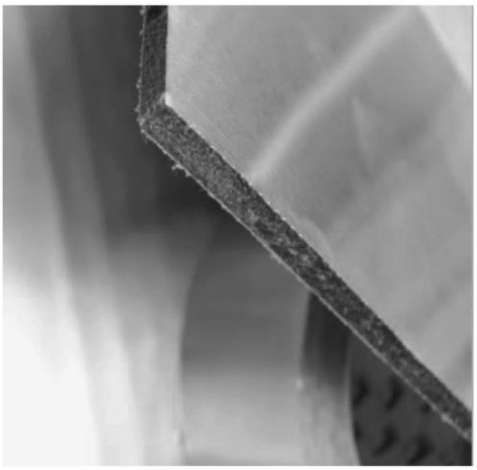

Fig. 5.1. Wallboard developed by *DuPont de Nemours* Society (Figure from [66]).

For cooling applications, a combination of night ventilation, AC unit and energy price based control system was used. The results indicated an impressive 73 % energy saving and 67 % cost saving over one week measurement period. However, in the same study it was indicated that if a proper control strategy is not used the same combination of systems can also lead to an increase in energy consumption.

PCM integration into external walls can help to lower heat flux from exterior to interior of a room. This is particularly important in lightweight wooden or metal frame walls.

Carbonari et al. [70] performed an experimental and numerical study on prefabricated sandwich panels with integrated PCM layer. The mathematical model demonstrated good agreement with measured values. The team found that the incorporation of PCM materials in sandwich type external walls allows them to thermodynamically resemble high thermal mass walls while keeping the advantages of a sandwich wall (fast and easy installation and low weight).

Evers et al. [71] carried out a numerical study for lightweight frame wall with integrated PCMs. The team found that the peak heat flux was reduced by 9.2 % and the daily average heat flow reduced by 1.2 %.

An external wall with a composition of insulation-PCM-insulation (resistance-capacity-resistance) was numerically tested by Halford and Boehm [72]. The proposed wall model was intended for cooling peak load shifting. The models predicted a 11–25 % of peak load reduction over a scenario with only mass but no PCM inside the wall and 19–57 % of peak load reduction over a scenario with only insulation.

Alawadhi [73] performed numerical study on bricks with cavities filled with PCM. The author concluded that if three PCM cylinders are located in the middle part of the brick, the heat flux can be reduced by approximately 18 %.

Alawadhi and Alqallaf [74] studied a roof with cone shaped PCM pockets in the roof slab and concluded that the heat flux to indoor space can be reduced by approximately 39 %.

5.2. Active PCM Thermal Storage Systems

Active thermal storage systems typically include some active energy delivery or extraction mechanism that serves as a heat exchanger between the room and the PCM storage or between the PCM and a cooling or heating energy source.

PCM to air heat exchangers are probably the most researched type of active PCM thermal storage systems. These types of systems allow to control the energy flow in and out of PCM storage as well as fully utilize the energy storage potential by selecting proper PCM layer thickness [75]–[77]. This allows to overcome low thermal conductivity and to access all stored energy. Cooling and heating energy delivery to conditioned spaces can also be controlled.

Jaworski et al. [78], [79] performed an experimentally validated numerical study of a ceiling mounted PCM to air heat storage integrated into a ventilation system. The heat exchanger was constructed of a micro-encapsulated PCM and gypsum composite. The thermal storage was designed to withstand an eight hour 30 °C heat wave of outdoor air flow through the heat exchanger after a 16-hour recharging period with outdoor air temperature of 16 °C. During the heat wave period the supply air temperature did not exceed 24 °C and the melting temperature of the used PCM was 22.8 °C.

Borderon et al. [80] performed an exhaustive simulation study for a 100 m² residence cooled with ventilation air from a PCM to air heat exchanger storage system. The simulation study was performed for four locations in France: Lyon, Nice, Trappes, Carpentras. The team found that with a 700 kg PCM thermal storage it is possible to limit the overheating in the residence to under 8 % if 26 °C is considered the limit. The main issue the team reported was the inability to fully recharge the PCM storage during warm nights that resulted in increased fan energy.

Another commonly researched method is to use thermally activated building structures (TABS) or **cooling units with integrated PCMs such as ceiling panels** with PCM layers or slabs with capsulated PCMs, however, this system is not widely commercialized. Aforementioned units generally are thermally activated with a hydronic circuit, and cooling energy is supplied from a central cooling plant with a passive or active cooling energy generator.

The most common application is to use a hydronic circuit which is located near or immersed in the PCM layers of a cooling panel or a slab.

Koschenz and Lehmann [56] developed a thermally activated ceiling panel for cooling (Fig. 5.2) and also did numerical analyses in *TRANSYS*. The developed panel had a thermal storage capacity of 0.3 kWh/m² and was composed of microencapsulated PCM (Heptadecane-based paraffin with phase change temperature of around 22 °C) and gypsum composite. To enhance the thermal conductivity of the panel, it was supplemented with aluminium fins. The measured average heat conductivity of the panel was 1.1–1.2 W/(m·K), the density was 1030 kg/m³, and the amount of microencapsulated PCM was 13.3 kg/m². According to the test results the panel withstood a 40 W/m² heat flux for 7.5 hours before the PCM transitioned to a liquid state.

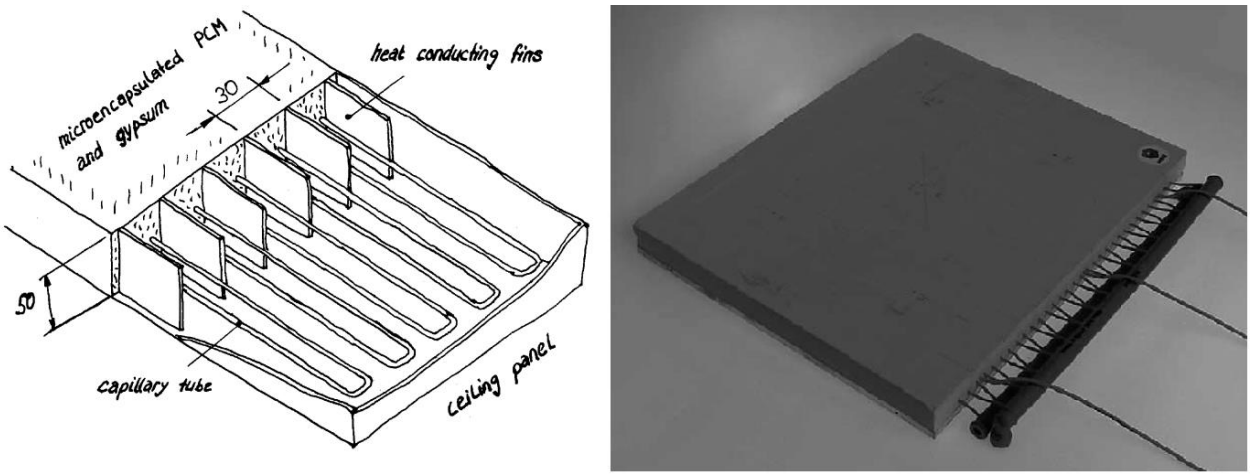

Fig. 5.2. PCM cooling panel developed by Koschenz and Lehmann [56].

Weinlander et al. [81] developed and tested two types of ceiling panels (Fig. 5.3) with microencapsulated PCM layer above the hydronic circuit – the first type of cooling panel; and below the hydronic circuit – the second type of cooling panel. The measured passive cooling powers were from 8 W to 17 W per square meter of ceiling area for globe temperatures from 24 °C to 27 °C. Passive cooling power for 26 °C globe temperature was between 10–15 W/m² depending on the heat load. The phase change temperature for the investigated PCM was between 22 °C and 24 °C.

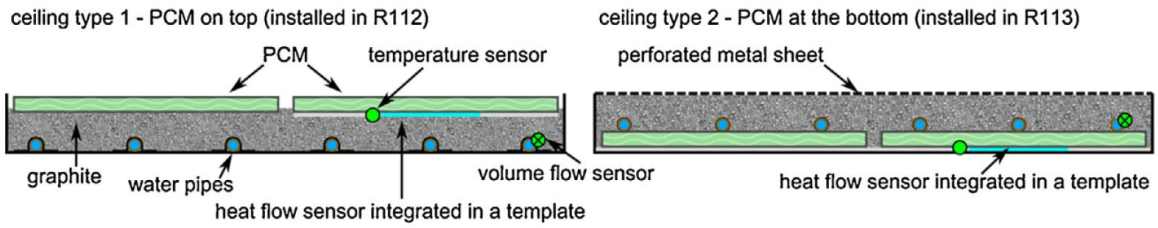

Fig. 5.3. Cooling panels developed by Weinlander et al. [81].

Similar approach was tried by a Latvian researchers' team, Rucevskis et al. [82]–[84], that performed an extensive numerical analysis using CFD modelling for steel panel with liquid PCM. This type of PCM panel is also investigated in the experimental part of this Thesis where results generated by an experimentally calibrated numerical model developed in *IDA ICE* were compared to CFD modelling results reported by Rucevskis et al. [83], [84] (See Chapters 7 and 8).

The estimated thermal storage capacity for the panel was 0.59 kWh/m² panel area and the phase change temperature was around 23 °C. The team modelled PCM panels with 25 mm thickness and 100 % coverage of the ceiling for an eight-day period. The maximum room temperature for the analysed period is nearly 7 °C lower if thermally active PCM panels are used and only 2 °C lower if passive PCM panels are used. It was also concluded that in the case of thermally active panels only 66 % of the thermal storage capacity was used, but in the case of passive PCM panels after 85 hours the PCM storage had been completely depleted and did not solidify during the following simulation period (Fig. 5.4).

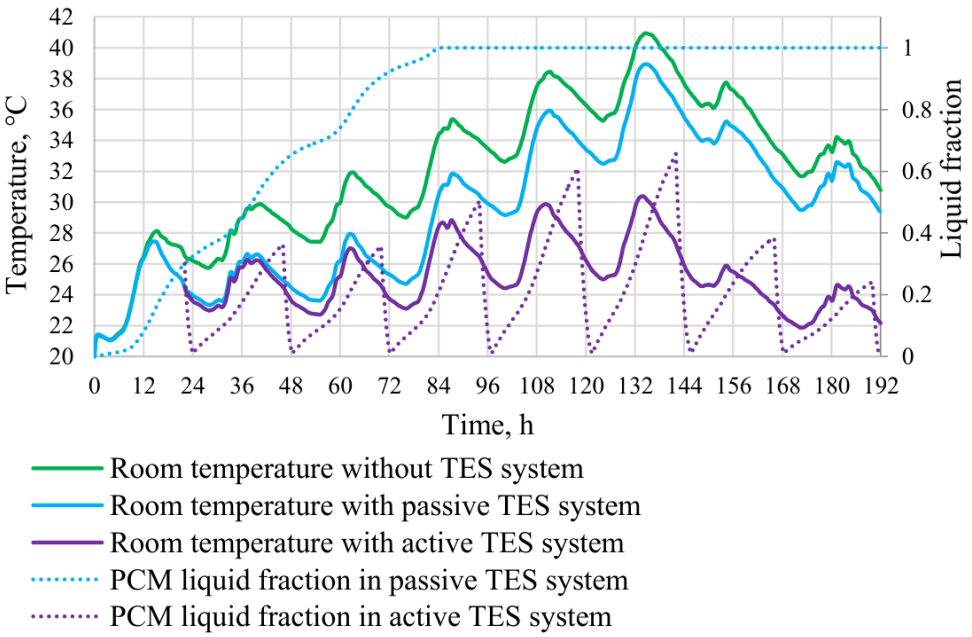

Fig. 5.4. Temperature and PCM liquid fraction for PCM storage simulated by Rucevskis et al. [82]–[84].

6. REVIEW OF HEAT TRANSFER THEORY

Application of newly developed HVAC system requires in-depth understanding of heat transfer fundamentals in order to understand the governing processes and develop calculation methods and simulation models for these components. This chapter is dedicated to the fundamentals of heat transfer in relation of HVAC systems (including PCM cooling panels).

There are three fundamental types of heat transfer in HVAC systems – conduction, convection and radiation.

Conduction takes place in solids, liquids, stationary gases and vapour boundary layers through the collisions of molecules and atoms. Conduction can be described with Fourier's law of heat conduction that was formulated in 1822 and can be represented with Equation (6.1) for one-dimensional steady-state case with constant specific heat conductivity.

$$q_x = -\lambda \frac{\mathrm{d}T}{\mathrm{d}x} = \frac{Q_x}{A}, \tag{6.1}$$

where q_x – the specific heat transfer due to conduction in direction x, W/m²;

λ – thermal conductivity, W/(m·K);

$\frac{\mathrm{d}T}{\mathrm{d}x}$ – the temperature gradient, K/m;

Q_x – total heat flow in direction x over area A (Fig. 6.1), W;

A – area, m².

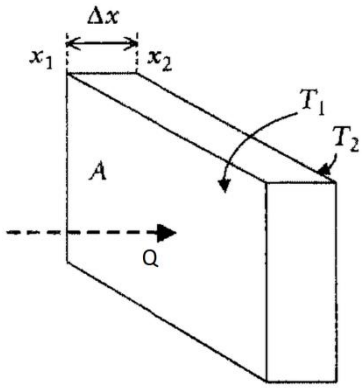

Fig. 6.1. One dimensional heat flow [85].

Integration of Equation (6.1) gives Equation (6.2).

$$Q \int_{x_2}^{x_1} \mathrm{d}x = -\lambda A \int_{T_2}^{T_1} \mathrm{d}T \;\rightarrow\; Q = -\lambda A \frac{\Delta T}{\Delta x}, \tag{6.2}$$

where Q – heat flow, W;

x_1 – coordinate of surface 1, m;

x_2 – coordinate of surface 2, m;

T_1 – temperature of pane 1, m;

T_2 – temperature of pane 2, m;

ΔT – temperature difference across the layer, m;

Δx – thickness of the layer, m.

Convection occurs between a surface and a moving liquid. Although the heat transfer in the boundary takes place in the form of conduction, the energy transfer with matter governs the process.

Convection can be divided into two types: natural and forced. Natural convection is self-induced because the density of a liquid is temperature dependent and cooler parts of the liquid with higher density are pulled down by the gravity and parts with lower density are displaced up. Forced convention is caused by an external force that causes the liquid to move near a convective surface.

Convection between a surface and a fluid can be described with Newton's law of cooling:

$$q_{\text{conv}} = h_{\text{conv}} \Delta T, \tag{6.3}$$

where q_{conv} – specific heat flow between a fluid and a surface, W/m²;

h_{conv} – convective heat transfer coefficient, W/(m²·K);

ΔT – temperature between the surface and the liquid over a long distance (average temperature of the liquid flow), K.

However, in practical applications the determination of the convective heat transfer coefficient and convection in general is very complex, and it is practically impossible to theoretically describe it. In order to practically estimate convective heat transfer, empirical formulas must be used.

Convective heat transfer coefficients for practical applications can vary in orders of magnitude depending on liquids used and properties of the system, typical values are illustrated in Table 6.1.

Table 6.1

Typical Convective Heat Transfer Coefficients

Type of convection, W/(m²·K)	Literature source		
	ASHRAE Fundamentals [86]	Goodfellow and Tahti [85]	Stoecker and Jones [87]
Free convection, gases	2 to 25	3.5 to 50	5 to 25 (air)
Free convection, liquids	10 to 1000	–	50 to 100 (water)
Forced convection, gases	50 to 20 000	10 to 500 (air)	10 to 200 (air)
Forced convection, liquids	2500 to 100 000	100 to 5000	50 to 100 000 (water)

In order to approximate the convective heat transfer in a thermodynamic system, Nusselt number Nu is introduced. The relation of the Nusselt number and convective heat transfer coefficient can be expressed with Equation (6.4).

$$Nu = \frac{h_{\text{conv}} L}{\lambda} \rightarrow h_{\text{conv}} = \frac{Nu\lambda}{L}, \tag{6.4}$$

where Nu – Nusselt number;

L – characteristic length (pipe diameter or hydraulic diameter $d_{\text{h}} = \frac{4A}{P}$, where A is the cross section area and P is the whetted perimeter), m.

For forced convection, Nusselt number is a function of Reynolds number and Prandtl number $\left(Nu = f(Re, Pr)\right)$, and for free convection, Nusselt number is a function of Grashof number and Prandtl number ($Nu = f(Gr, Pr)$). Pr is the Prandtl number (Equation (6.5)) and Gr is the Grashof number (Equation (6.6)) and Re is the Reynolds number (Equation (6.7)).

$$Pr = \frac{v\rho c_p}{\lambda}, \tag{6.5}$$

where Pr – Prandtl number;

v – kinematic viscosity, m²/s;

ρ – density of the fluid, kg/m³;

c_p – heat capacity of the liquid, J/(kg·K).

$$Gr = \frac{g\beta\Delta T L^3}{v^2}, \tag{6.6}$$

where Gr – Grashof number;

g – the acceleration due to earth's gravity, 9.80665 m/s²;

β – coefficient of thermal expansion, 1/K.

$$Re = \frac{uL}{v}, \tag{6.7}$$

where Re – Reynolds number;

u – velocity of the flow, m/s.

For practical calculations there are numerous empirical correlations for $Nu = f(Re, Pr)$ and $Nu = f(Gr, Pr)$ functions for generalized cases that can be found in literature.

Radiation energy transfer is governed by:

- Planck's law of radiation that describes radiation energy distribution in a spectrum;
- Stefan–Boltzmann law that describes the energy emitted by a black body;
- Wien's law that describes the product of maximum wavelength (or at which wavelength radiation energy peaks for different temperatures).

However, Stefan–Boltzmann law and Wien's law can be derived from the more fundamental Planck's law of radiation.

In more simple terms, Planck's law of Radiation describes the location of each point on the distribution lines in Fig. 6.2, Stefan–Boltzmann law describes the area each spectral line forms with abscissa axis in Fig. 6.2 (that also is the total energy emitted), and Wiens's law describes the extrema (peak) of each spectral line of Fig. 6.2.

Stefan–Boltzmann law for engineering calculations must be used while keeping in mind that the law describes the total energy radiation and the emissivities given in the literature are the total values over the whole spectrum.

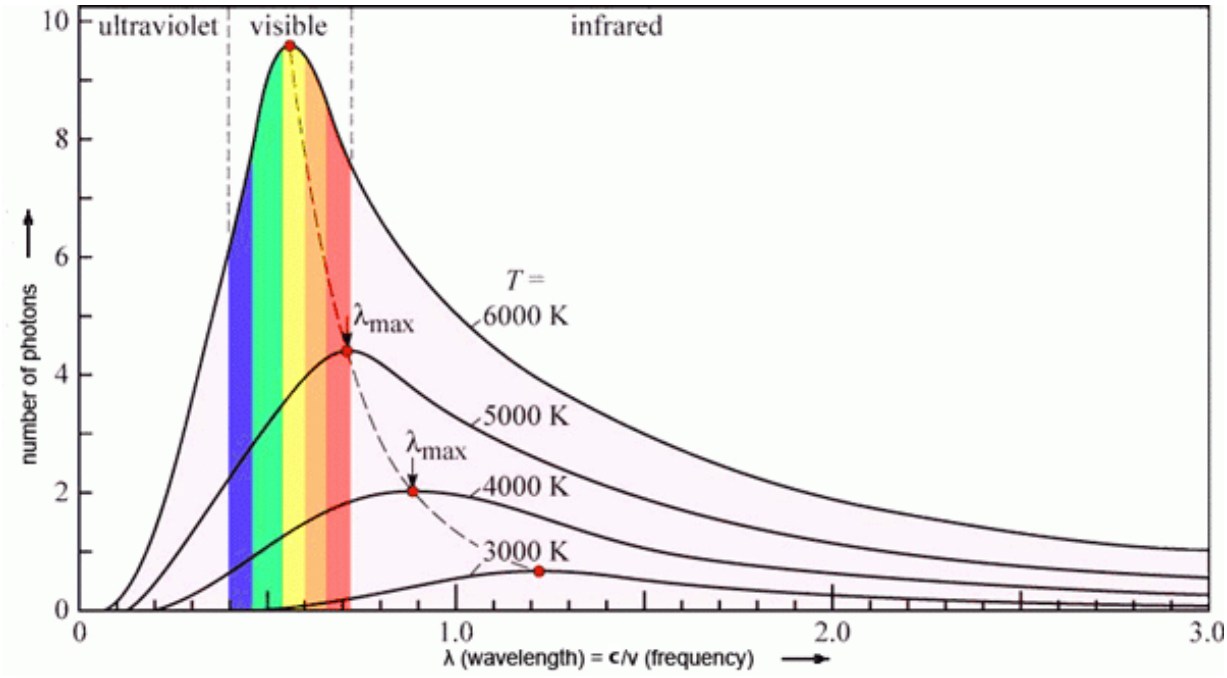

Fig. 6.2. The spectral distribution of black body radiation (Figure from [88]).

These fundamentals are required to develop new latent thermal storage systems and apply existing systems. They are essential for developing mathematical representations or simulation models of physical components to predict the behaviour of these components for the specific case of interest.

7. METHODOLOGY

The experimental part of this Thesis focuses on the development and experimental verification of an equation based simulation model for a PCM cooling panel – a stainless steel container filled with PCM and an integrated hydronic circuit. This PCM panel was previously developed in the scope of a research project *No.1.1.1.1/16/A/007 "A New Concept for Sustainable and Nearly Zero-Energy Buildings"*.

The developed model may further be used for faster, simpler, more accurate energy modelling and sizing of heating, ventilation and air conditioning systems.

There are four main objectives of this study.

- To indirectly measure the heat loss coefficient of the experimental chamber at thermal equilibrium conditions using the temperature measurements inside the chamber, temperature measurements of the surrounding environment and measurements of the thermal energy supplied inside the chamber.
- To perform a series of experiments with PCM panels in a test chamber using variable internal heat gains for a case without a cooling panel and a case with a cooling panel that is connected to a cooling water flow.
- To validate the developed PCM cooling panel simulation model using *IDA ICE 4.8* [89], [90] simulation software and measurements from the test chamber.
- To perform a comparative simulation study using the validated simulation model of the PCM panel and compare it with the results obtained in a previous CFD simulation study carried out by Rucevskis et al. [83], [84].

7.1. Experimental Set-Up

To carry out laboratory tests, an experimental chamber was constructed for this experiment (Fig. 7.1).

The heat loss coefficient was indirectly measured by inserting a heat source with a heating capacity of 90.1 W inside the chamber. The temperatures inside and outside of the chamber were measured. When a thermal equilibrium was reached, the heat loss coefficient (W/K) of the chamber was calculated using the temperature difference between the inside and outside of the chamber and the power of the heat source. The calculated heat loss coefficient of the chamber was H_t = 8.06 W/K.

The chamber was equipped with eight temperature/humidity (Fig. 7.1) probes at various locations of the chamber:

- T1 – surface temperature sensor on the upper face of the panel;
- T2 – surface temperature sensor on the lower face of the panel;
- TH3 – air temperature and humidity sensor outside the chamber;
- T4 – surface temperature sensor for the supply pipe of the panel;
- T5 – surface temperature sensor for the return pipe of the panel;
- TH6 – air temperature and humidity sensor in the middle part of the chamber;

- TH7 – air temperature and humidity sensor in the lower part of the chamber;
- TH8 – air temperature and humidity sensor in the upper part of the chamber.

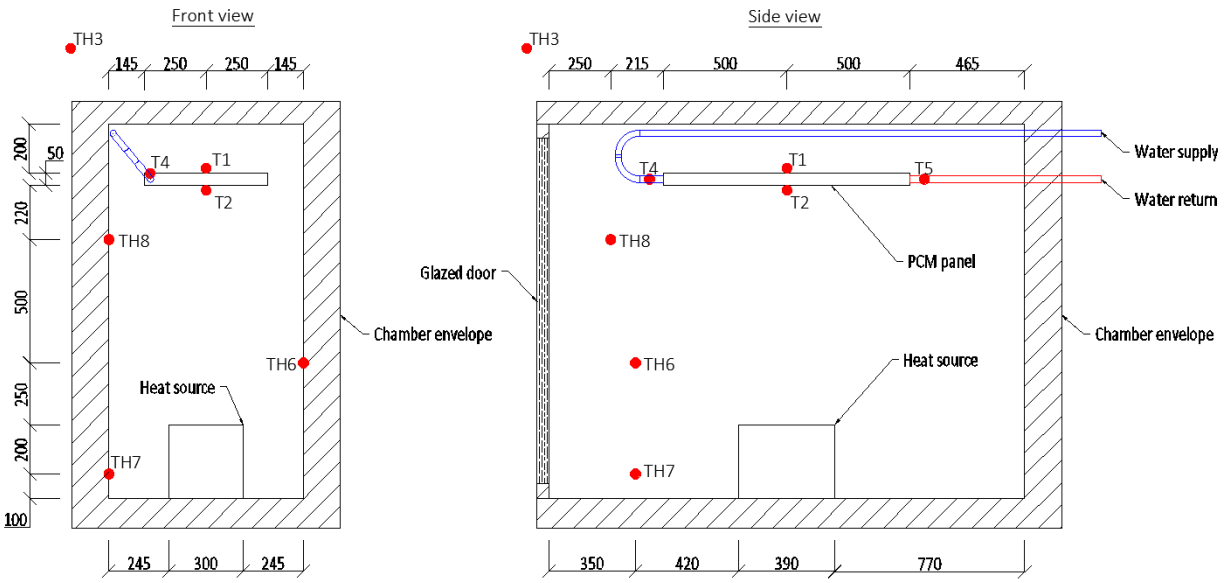

Fig. 7.1. Test chamber used for the study.

The cooling panel consists of a stainless-steel container with internal hydronic circuit (Fig. 7.2). 80 % of panel volume was filled with *RUBITHERM© RT22HC* [91] phase change material. According to the technical properties provided by the manufacturer, the heat storage capacity of the PCM is 190 kJ/kg in the temperature range from 14 °C to 29 °C, which in theory would provide the panel a heat storage capacity of approximately 1.48 kWh/m² panel area. However, the operational temperature range of the panel typically ranges from 19 °C to 24 °C. That ensures a useful heat storage capacity of the PCM only 140 kJ/kg and the heat storage capacity of 1.09 kWh/m² panel area.

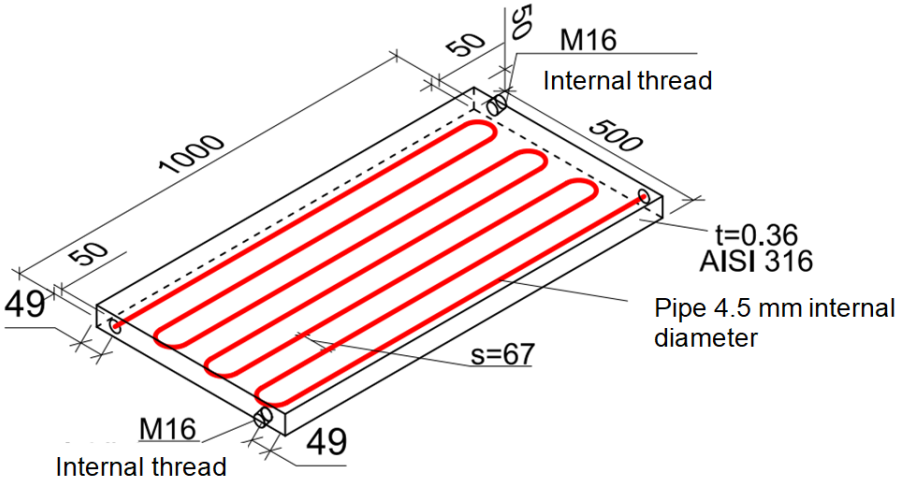

Fig. 7.2. Cooling panel (dimensions in mm).

Moreover, according to the manufacturer's data [91] there is an inconsistency because the total phase change enthalpy over the phase change range (14 °C to 29 °C) is different for melting [208 kJ/(kg·K)] and solidification [197 kJ/(kg·K)]. The partial enthalpies used for the

simulation model were slightly adjusted for numerical reasons to have the same phase change enthalpy for both melting and solidification. The measured data provided by the manufacturer and the corrected data used for the simulation model can be observed in Fig. 7.3.

The cooling panel had an internal hydronic circuit that consisted of stainless-steel pipes with 4.5 mm internal diameter and 67 mm gap between pipes. A heat source was introduced to simulate the performance of the cooling panel. The hourly average heat gains are visualized in Fig. 7.4.

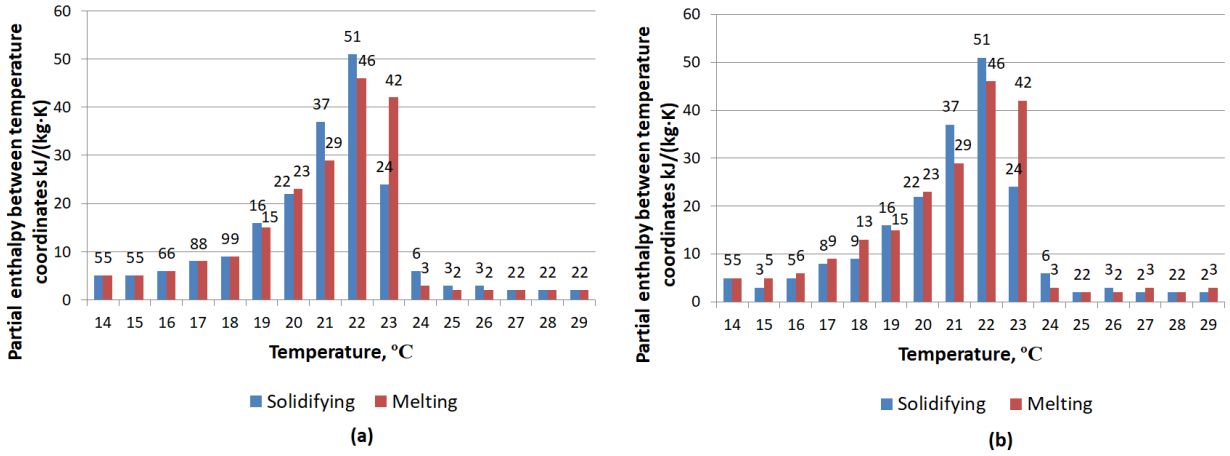

Fig. 7.3. Adjusted (a) and measured (b) partial enthalpy model of the PCM.

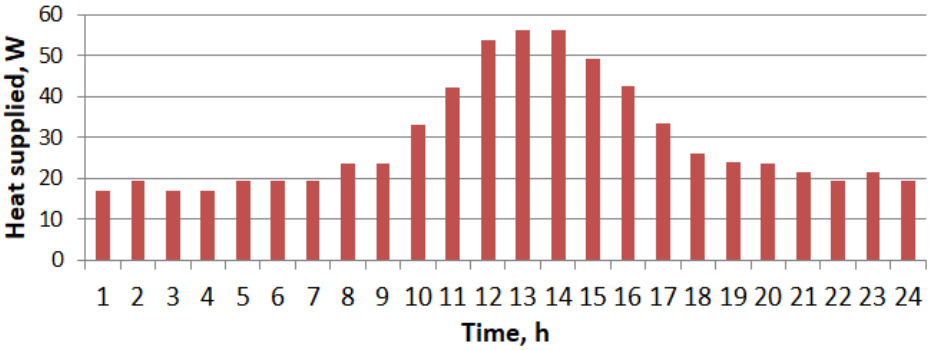

Fig. 7.4. Heat supply schedule.

A simulation model of the experimental system (test chamber and the surrounding room) was developed in *IDA ICE 4.8*.

The measured heat loss coefficient H_t was used to fine-tune envelope *U*-values of the simulated test chamber. During the simulation runs, the temperature of the surrounding environment in the simulation model was kept the same as the measured surrounding room temperature during the experiments. Only the radiant heat exchange between the surroundings and the chamber could not be precisely modelled, because the surface temperatures and the short and long wave radiation sources (windows) were not measured during the experiments.

The cooling panel was modelled as a hydronic circuit thermally connected to PCM layers and container wall which was then exposed to the simulated zone with combined radiant and convective heat transfer coefficients.

Total or combined radiant and convective heat transfer coefficients were adjusted during the model validation to 100 W/(m²·K) (a relatively high value for natural convection). However, these coefficients did not significantly influence the heat transfer from the hydronic circuit as it is mostly dependent on the relatively low heat conductivity of the PCM material [λ = 0.2 W/(m·K)].

The PCM layer was modelled by applying a mathematical model of different temperature – enthalpy relations during melting and solidification to consider the effect of hysteresis. The model consists of 16 partial material enthalpies between temperature coordinates for a temperature range from 14 °C to 29 °C, which is consistent with thermal properties of *RUBITHERM© RT22HC* [91] phase change material.

The hydronic circuit in the model was approximated as a layer that delivers cooling energy to PCM material based on a heat transfer coefficient and temperature difference. Heat transfer coefficient fluid to PCM material was calculated with the *U-NORM 2012-2* software that uses the finite difference model to calculate the heat flow and temperature distribution for two-dimensional and three-dimensional cases based on the energy balance.

The calculation procedure and the pipe circuit approximation to a layer was performed according to the methodology described in EN 15377-1 [92]. *U-NORM* software was used to calculate the extra thermal resistance between average water temperature inside the circuit and the average temperature of the heat conducting layer – the R_t value. The relative temperature distribution and calculation principle is visualised in Fig. 7.5, where T_v is the average water temperature in a hydronic circuit, R_t is the additional thermal resistance for approximating piping circuit to a fictive surface, T_c is the average temperature for the heating or cooling layer, T_1 T_2 and R_1 R_2 are the surface temperatures and layer thermal resistances that are calculated by *IDA ICE* solver using the PCM mathematical model and finite difference models. The calculated heat transfer coefficient is $1/R_t$ = 11.8 W/(m²·K).

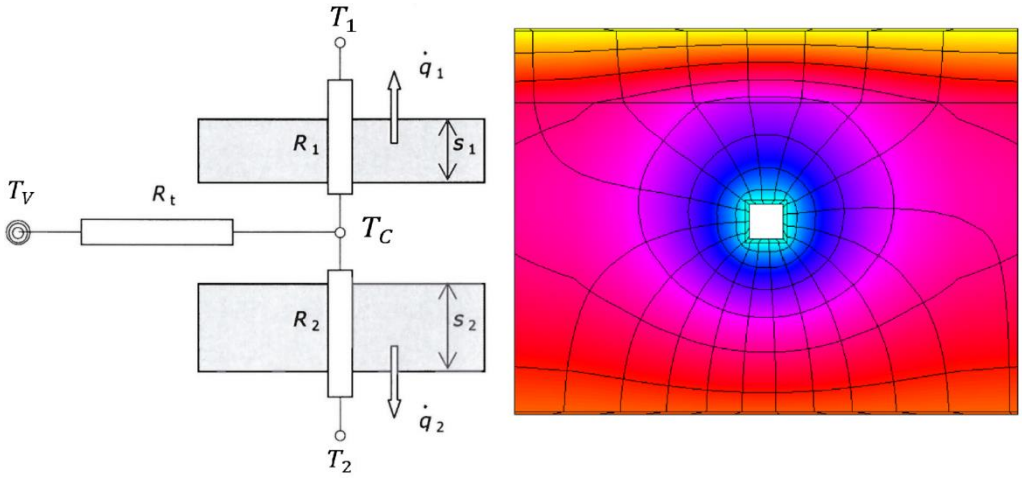

Fig. 7.5. Resistance network in embedded water based surface heating and cooling systems [92] and relative temperature distribution in the PCM panel.

7.2. Simulation Model for Performance Modelling

In order to model the PCM cooling panel performance for more realistic cooling application, it was decided to replicate a simulation model set-up from the previous study that was conducted by Rucevskis et al. [83], [84].

This particular study was chosen because of a very similar type of PCM cooling panel used and the same PCM material. Rucevskis et al. [83], [84] performed the simulation using CFD (*Fluent*). The general simulation set-up used by Rucevskis et al. [83], [84] is represented in Fig. 7.6. As external boundary conditions the team used outdoor air temperature and solar radiation for a typical eight-day summer period in Riga, Latvia.

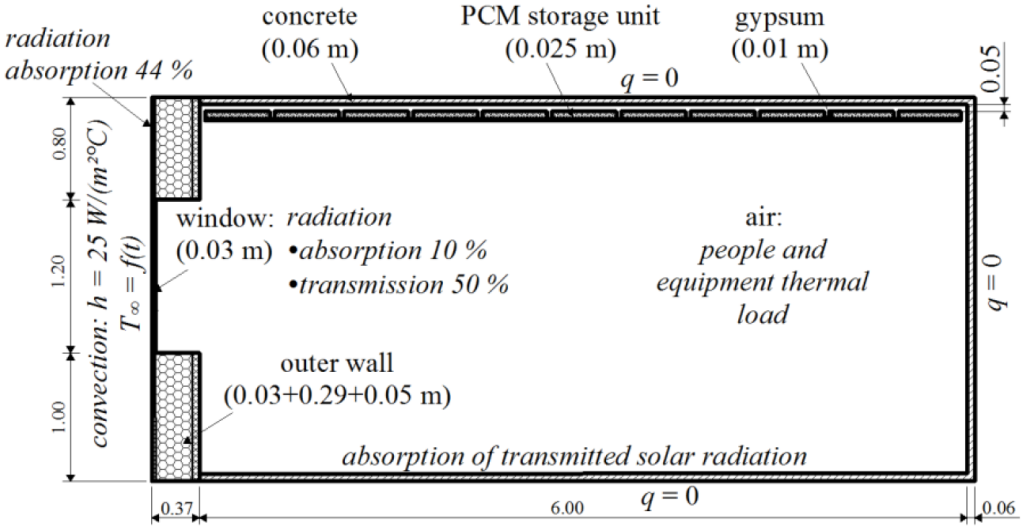

Fig. 7.6. Simulation set-up used by Rucevskis et al. [83], [84].

8. RESULTS AND DISCUSSION

8.1. Verification of the Simulation Model

After adjusting the heat loss coefficient of the test chamber envelope according to the measured value, a simulation was run for seven consecutive days and compared with the measurement data from the same time period. The simulated temperature inside the chamber corresponded relatively well with the measurements – the maximum deviation between the measured value and the simulated value was less than 1 °C. One of the possible explanations for the discrepancy that arose can be the fact that the room where the experiment took place had significant glazing. Moreover, due to technical limitations the radiant temperature and the radiation from the glazed surfaces was not measured and, therefore, could not be accounted for in the simulation model. This would also explain why the first two days the measured and simulated data correspond almost perfectly, but the following days begin to drift apart (Fig. 8.1). This may be due to the fact that during the experiment the first two days were mostly cloudy and the following days were mostly sunny.

Measured and simulated values over the investigated period had a relatively high Pearson correlation coefficient of 0.98 and relatively low root mean square error (RMSE) of 0.53 °C.

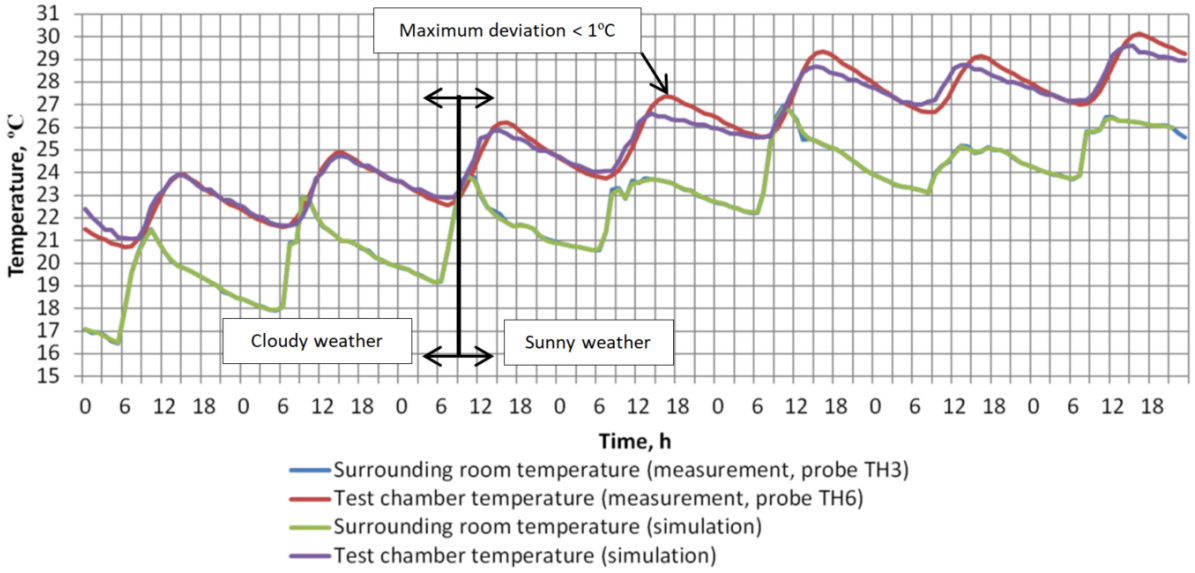

Fig. 8.1. Measurements versus simulation-case without a PCM cooling panel.

8.2. Simulation Model with a PCM Cooling Panel and Cooling Water Connection

After making sure that the test chamber envelope model had a reasonable agreement between the simulated and measured values by fine-tuning the chamber H_t value according to measurements, the PCM panel could be simulated. An 11-day period was chosen for the simulation (Fig. 8.2).

With the introduction of a PCM cooling panel, the difference between the simulated and measured values increased to a maximum of 2 °C and the RMSE increased to 1.01 °C. This disagreement can partly be explained with the uncertainty of the temperature sensors and the fact that the radiant heat exchange between the test chamber and surrounding room was not properly modelled. However, the simulation model always calculates a higher temperature than actually measured in the test chamber. However, when average temperatures over the 11-day period were compared, the agreement between the measured and simulated data was better. The average temperature in the simulation was 26.4 °C versus 25.2 °C for the measured data, which results in a discrepancy of 1.2 °C.

In general, the agreement between simulated and measured values is relatively good if compared to similar studies where simulation results of a dynamic simulation software are compared to measured values.

A team from Austria did a validation study [93] for four different dynamic simulation tools, including *IDA ICE*, and compared the results to measured values. The maximum deviation ranged from ~3.5 °C to ~4.7 °C, and RMSE ranged from ~0.5 °C to ~2.5 °C for a yearly simulation carried out with several different simulation tools.

Furthermore, a team from Italy conducted a similar study using *IDA ICE* [94] with two test chambers and a passive PCM thermal storage. When the measured values were compared to simulated values for an eight-day period, the RMSE for the chamber with no PCM storage was 2.50 °C and the RMSE for a chamber with a PCM storage was 1.83 C.

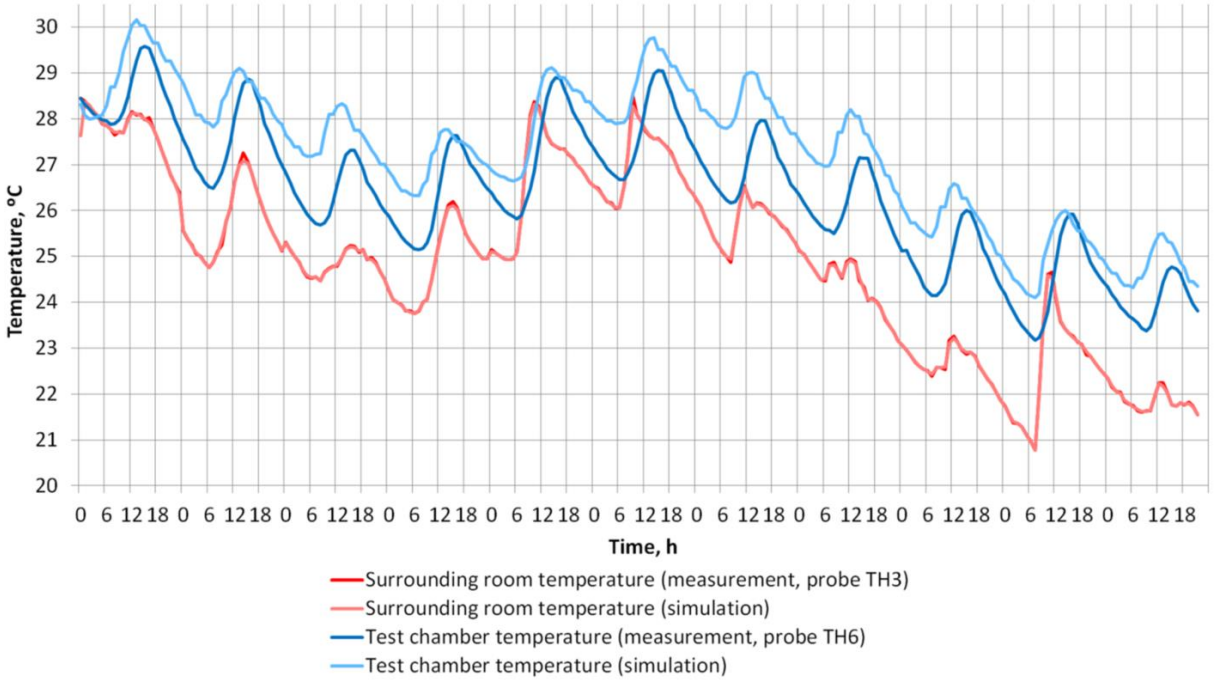

Fig. 8.2. Air temperature measurements versus simulation – the case with a PCM cooling panel

8.3. Performance Modelling – Comparative Case

Results from both simulations provided very similar results (Fig. 8.3). For the case with no cooling panels the maximum room temperature reached in the CFD simulation was 40.8 °C vs. 41.8 °C temperature in the *IDA ICE* simulation. In the case with thermally activated PCM panels, the maximum temperature reached was 30.4 °C in the CFD simulation, whereas in the *IDA ICE* it was 33.0 °C.

When comparing the average temperature over the simulated period, the agreement between both studies was more significant. Average temperature for the case with no PCM cooling panels was 32.1 °C for the CFD simulation and 31.5 °C for *IDA ICE* simulation (0.6 °C difference). In the case with the active PCM cooling panels, the average temperature for the CFD simulation was 25.2 °C, and 24.5 °C for the *IDA ICE* simulation (0.7 °C difference). The RMSE, when *IDA ICE* simulation was compared to CFD, is 1.13 ℃ for the case with no PCM panel and 1.31 °C for the case with thermally active PCM panel.

The reached agreement between CFD simulation and dynamic simulation in *IDA ICE* is similar as reported in other studies [93].

The difference of simulated results in *IDA ICE* and CFD for average temperatures is insignificant (less than 1 °C), and it can be considered negligible for annual energy simulations. However, the disagreement for peak values can reach approximately 2.5 °C.

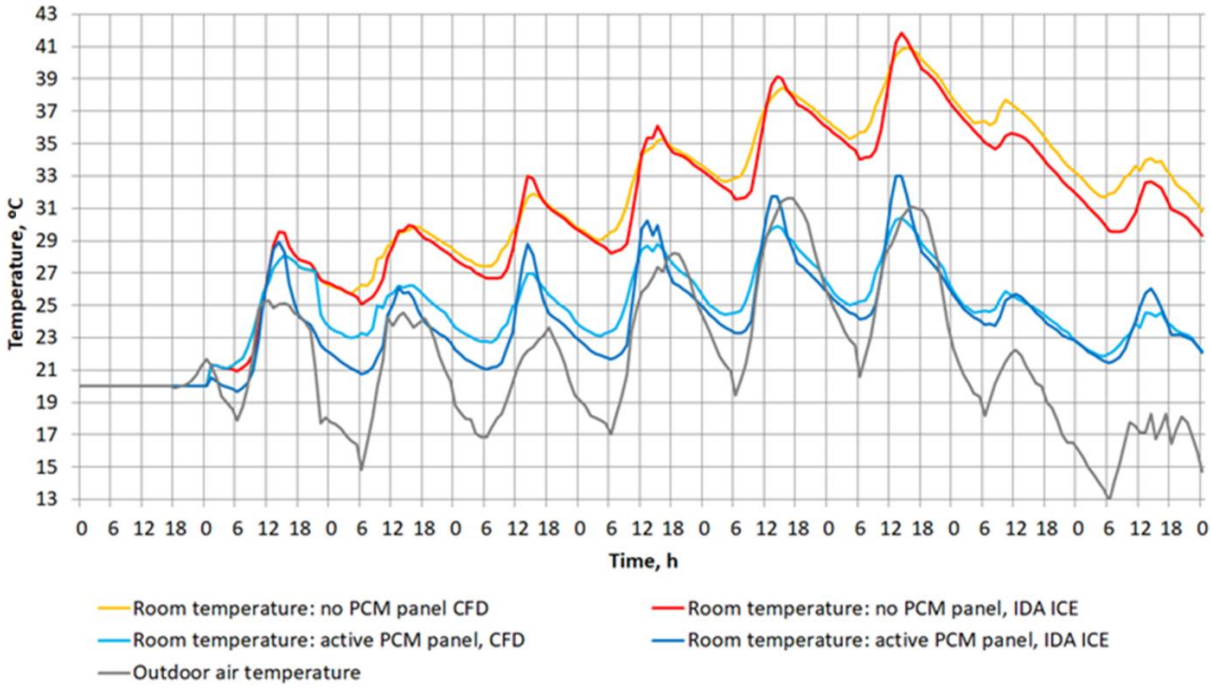

Fig. 8.3. Comparison of predicted room temperatures in *IDA ICE* and CFD simulations.

8.4. Summary of the Results

Altogether four simulation cases were simulated.

The first simulation of the test chamber without a PCM cooling panel was performed to confirm that in general the chamber in the simulation software is a valid representation of the

actual set-up. During the simulation it was acknowledged that due to the technical limitations it was not possible to account for the long-wave and the short-wave radiation from windows in the laboratory room. Throughout the first two days when the weather was cloudy the measured and simulated values agreed nearly perfectly, but begun to drift apart afterwards during the sunny weather.

The second simulation of the test chamber with a PCM cooling panel was performed in order to validate the results generated by the developed simulation model of the PCM cooling panel. With the introduction of the panel the maximum deviation and RMSE increased (see Table 8.1). However, these values were equal or better than reported in other similar studies.

The third and fourth simulation cases where the developed model was compared with the results from the CFD simulation study were performed to evaluate the performance for a more practical situation. The maximum deviation and RMSE in these cases were similar with the values acquired in the first and second case (Table 8.1). It can be concluded that the values acquired in the second and forth case describe the actual accuracy of the developed model.

Table 8.1

Summary of Statistical Indicators of the Simulation Results

Statistical indicator	Value reached in this study	Values reached in other similar studies
Simulated values against measurements – the case without a PCM panel		
$D_{\max}$	less than 1 °C	–
D_{avg}	–	–
r	0.98	–
$RMSE$	0.53 °C	–
Simulated values against measurements – the case with a PCM panel		
$D_{\max}$	2.2 °C	Nageler et al. from ~3.5 °C to ~4.7 °C [93]; Cornaro et al. 2.5 °C [94]
D_{avg}	1.2 °C	–
r	0.95	
$RMSE$	1.01 °C	Nageler et al. from ~0.5 °C to ~1.8 °C [93]; Cornaro et al. 1.83 °C [94]
Simulation model against previous CFD study – the case without a PCM panel		
$D_{\max}$	1 °C	–
D_{avg}	0.6 °C	–
r	0.98	–
$RMSE$	1.1 °C	–
Simulation model against previous CFD study – the case with a PCM panel		
$D_{\max}$	2.6 °C	–
D_{avg}	0.7 °C	–
r	0.93	–
$RMSE$	1.3 °C	–

8.5. Limitations of the Developed Model

Since the developed model utilises a combined radiant and convective heat transfer coefficient and the estimated heat exchange in the experimental set-up is 80 % convective and 20 % radiant, the model shall be applied for similar conditions.

The panel was validated for 40 mm PCM thickness (20 mm above hydronic circuit and 20 mm below). Internal buoyancy and change of volume during phase transition are not modelled. The PCM layer is not modelled with finite difference model but as uniform layer with evenly distributed state of the PCM material and evenly distributed temperature. PCM thickness greater than 20 mm above the cooling circuit and 20 mm below the cooling circuit shall not be used when applying this model.

The hydronic circuit is modelled according to the EN 15377-1 [92] with fixed heat transfer that accounts for equivalent heat transfer from water to an imaginary layer located in the middle of the PCM. If the properties of the hydronic circuit and PCM significantly differ from the values used in this study, the R_t value shall be recalculated to suit the properties of the modelled system. Particular attention shall be paid to the thermal conductivity of PCM and situations where the liquid inside the cooling circuit is not pure water (water with antifreeze additives) or the flow is not turbulent.

9. CONCLUSION

This Thesis represents an original research that consists of a state of art literature review and an experimental study.

The experimental study consists of a description of the developed equation based simulation model and series of experiments to validate and evaluate the performance of the model. The main advantage of the developed equation based simulation model over the CFD simulation is the ability to perform practical full building scale cooling, thermal comfort and energy simulations.

Statistical analyses are applied to evaluate the agreement between the results generated by the simulation model against experimental measurements and results generated in a CFD simulation previously carried out by other authors. The statistical indicators demonstrate that the reached accuracy of the developed model is adequate. The maximum deviation and RMSE is at least equal or better than reached in similar previous studies.

The accuracy reached by the developed simulation model can be considered suitable for application in construction industry if the limitations of the developed model are respected. Therefore, the hypothesis stated before the completion of the research: *"Experimentally validated equation based numerical simulation model of a hydronic cooling panel with integrated latent thermal storage can produce simulation results with accuracy suitable for application in construction industry to support other passive cooling technologies"* is confirmed.

After completion of the research, the following conclusions can be drawn.

1. Majority of the EU member countries have addressed the issue of overheating in NZEB and low energy buildings in their building codes.
2. Literature review indicates that a variety of reliable and industry-ready passive cooling technologies that can be supported by latent thermal storage systems.
3. Research of the field literature reveals that there are many PCM based thermal storage systems researched previously. PCM to air heat exchangers incorporated in ventilations systems and ceiling based PCM cooling panels can be perceived as the most promising systems.
4. According to the results it can be concluded that this type of numerical model indeed can produce simulation results with precision that is comparable with the results acquired in a CFD study.
5. The accuracy of the results acquired from the developed model is similar or more accurate than reported in similar studies.
6. The developed numerical model can be applied for practical use in construction industry for a whole building scale thermal comfort, cooling capacity and annual energy simulations.

BIBLIOGRAPHY

1. The Future of Cooling. *Futur. Cool.* **2018**, doi:10.1787/9789264301993-en.
2. Millers, R.; Korjakins, A.; Lešinskis, A.; Borodinecs, A. Cooling Panel with Integrated PCM Layer: A Verified Simulation Study. *Energies* **2020**, doi:10.3390/en13215715.
3. European Commission Proposal for a REGULATION OF THE EUROPEAN PARLIAMENT AND OF THE COUNCIL. *Eur. Union* 2020.
4. Eichhammer, W.; Fleiter, T.; Schlomann, B.; Faberi, S.; Fioretto, M.; Piccioni, N.; Lechtenbohmer, S.; Schuring, A.; Resch, G. *Study on the energy savings potentials in EU member states, candidate countries and EEA countries*; 2009.
5. Ovchinnikov, P.; Borodiņecs, A.; Millers, R. Utilization potential of low temperature hydronic space heating systems in Russia. *J. Build. Eng.* **2017**, *13*, doi:10.1016/j.jobe.2017.07.003.
6. Christensen, J.E.; Schiønning, P.; Dethlefsen, E. Comparison of simplified and advanced building simulation tool with measured data. In Proceedings of BS 2013: 13th Conference of the International Building Performance Simulation Association; 2013; pp. 2357–2364.
7. EPBD CA *2016 Implementing the Energy Performance of Building Directive (EPBD)*; 2016.
8. Vabariigi Valitsus Energiatõhususe miinimumnõuded 2015.
9. Latvijas republikas Minstru kabnets. Noteikumi par ēku energosertifikāciju, 2016.
10. Latvijas republikas Minstru kabinets. Noteikumi par Latvijas būvnormatīvu LBN 002-19 "Ēku norobežojošo konstrukciju siltumtehnika", 2019.
11. Latvijas republikas Minstru kabinets. Noteikumi par Latvijas būvnormatīvu LBN 231-15 "Dzīvojamo un publisko ēku apkure un ventilācija", 2015.
12. Stetiu, C.; Feustel, H.E. Phase-change wallboard and mechanical night ventilation in commercial buildings. *Lawrence Berkeley Natl. Lab.* **1998**.
13. Barzin, R.; Chen, J.J.J.; Young, B.R.; Farid, M.M. Application of PCM energy storage in combination with night ventilation for space cooling. *Appl. Energy* **2015**, *158*, 412–421, doi:10.1016/j.apenergy.2015.08.088.
14. Solgi, E.; Fayaz, R.; Kari, B.M. Cooling load reduction in office buildings of hot-arid climate, combining phase change materials and night purge ventilation. *Renew. Energy* **2016**, doi:10.1016/j.renene.2015.07.028.
15. Saffari, M.; de Gracia, A.; Ushak, S.; Cabeza, L.F. Passive cooling of buildings with phase change materials using whole-building energy simulation tools: A review. *Renew. Sustain. Energy Rev.* 2017.
16. Givoni, B. Evaporative Cooling Systems. *Passiv. Low Energy Cool. Build.* **1994**.
17. Givoni, B. Comfort, climate analysis and building design guidelines. *Energy Build.* **1992**, doi:10.1016/0378-7788(92)90047-K.
18. Givoni, B. Performance and applicability of passive and low-energy cooling systems. *Energy Build.* **1991**, doi:10.1016/0378-7788(91)90106-D.

19. SUSAN, R.; PHILIP, H.; ORR, J. Climate change and passive cooling in Europe. *Environ. FRfENDLY C. ES, Proce<idings PLEA '98* **1998**, 463–466.
20. Artmann, N.; Manz, H.; Heiselberg, P. Climatic potential for passive cooling of buildings by night-time ventilation in Europe. *Appl. Energy* **2007**, *84*, 187–201, doi:10.1016/j.apenergy.2006.05.004.
21. Meteonorm Global meteorological database for engineers, planners and education 2005.
22. Prozuments, A.; Vanags, I.; Borodinecs, A.; Millers, R.; Tumanova, K. A study of the passive cooling potential in simulated building in Latvian climate conditions. In Proceedings of the IOP Conference Series: Materials Science and Engineering; 2017; Vol. 251.
23. Meir, M. G.; Rekstad, J. B.; LØvvik, O. M. A study of a polymer-based radiative cooling system. *Sol. Energy* **2002**, doi:10.1016/S0038-092X(03)00019-7.
24. Eicker, U.; Dalibard, A. Photovoltaic-thermal collectors for night radiative cooling of buildings. *Sol. Energy* **2011**, doi:10.1016/j.solener.2011.03.015.
25. Péan, T.; Gennari, L.; Olesen, B. W.; Kazanci, O. B. Nighttime radiative cooling potential of unglazed and PV / T solar collectors : parametric and experimental analyses. In the Proceedings of the 8th Mediterranean Congress of Heating, Ventilation and Air-conditioning (climamed 2015); 2015.
26. Catalanotti, S.; Cuomo, V.; Piro, G.; Ruggi, D.; Silvestrini, V.; Troise, G. The radiative cooling of selective surfaces. *Sol. Energy* **1975**, doi:10.1016/0038-092X(75)90062-6.
27. Granqvist, C. G.; Hjortsberg, A. Surfaces for radiative cooling: Silicon monoxide films on aluminum. *Appl. Phys. Lett.* **1980**, doi:10.1063/1.91406.
28. Granqvist, C. G.; Hjortsberg, A. Radiative cooling to low temperatures: General considerations and application to selectively emitting SiO films. *J. Appl. Phys.* **1981**, doi:10.1063/1.329270.
29. Hossain, M. M.; Gu, M. Radiative cooling: Principles, progress, and potentials. *Adv. Sci.* 2016.
30. Berk, A.; Anderson, G. P.; Acharya, P. K.; Bernstein, L. S.; Muratov, L.; Lee, J.; Fox, M.; Adler-Golden, S. M.; Chetwynd, J. H.; Hoke, M. L.; et al. MODTRAN (TM) 5: 2006 update - art. no. 62331F. In *Algorithms and Technologies for Multispectral, Hyperspectral, and Ultraspectral Imagery XII Pts 1 and 2*; 2006 ISBN 0277-786Xr0-8194-6289-6.
31. Raman, A. P.; Anoma, M. A.; Zhu, L.; Rephaeli, E.; Fan, S. Passive radiative cooling below ambient air temperature under direct sunlight. *Nature* **2014**, doi:10.1038/nature13883.
32. Millers, R.; Korjakins, A.; Lesinskis, A. Thermally activated concrete slabs with integrated PCM materials. In Proceedings of the E3S Web of Conferences; 2019; Vol. 111.
33. Zhiyin Duan a; Changhong Zhan b; Xingxing Zhang a; Mahmud Mustafa a; Xudong Zhao a, n; Behrang Alimohammadisagvand c; Ala Hasan Indirect evaporative cooling: Past, present and future potentials. *Renew. Sustain. Energy Rev.* **2012**.

34. Amer, E. H. Passive options for solar cooling of buildings in arid areas. *Energy* **2006**, doi:10.1016/j.energy.2005.06.002.
35. Mavroudaki, P.; Beggs, C. B.; Sleigh, P. A.; Halliday, S. P. The potential for solar powered single-stage desiccant cooling in southern Europe. *Appl. Therm. Eng.* **2002**, doi:10.1016/S1359-4311(02)00034-0.
36. Jacovides, C. P.; Mihalakakou, G.; Santamouris, M.; Lewis, J. O. On the ground temperature profile for passive cooling applications in buildings. *Sol. Energy* **1996**, doi:10.1016/S0038-092X(96)00072-2.
37. Mihalakakou, G.; Santamouris, M.; Asimakopoulos, D. On the cooling potential of earth to air heat exchangers. *Energy Convers. Manag.* **1994**, doi:10.1016/0196-8904(94)90098-1.
38. Mihalakakou, G.; Santamouris, M.; Asimakopoulos, D. Use of the ground for heat dissipation. *Energy* **1994**, doi:10.1016/0360-5442(94)90101-5.
39. International Energy Agency Low Energy Cooling 2000.
40. Santamouris, M.; Kolokotsa, D. Passive cooling dissipation techniques for buildings and other structures: The state of the art. *Energy Build.* 2013.
41. Breesch, H.; Bossaer, A.; Janssens, A. Passive cooling in a low-energy office building. In Proceedings of the Solar Energy; 2005.
42. Pfafferott, J. Evaluation of earth-to-air heat exchangers with a standardised method to calculate energy efficiency. *Energy Build.* **2003**, doi:10.1016/S0378-7788(03)00055-0.
43. International Energy Agency Energy Conservation in Buildings and Community Systems, Annex 36 Case studies overview- UK1. **2003**, 117–122.
44. Fadejev, J.; Simson, R.; Kurnitski, J.; Kesti, J.; Mononen, T.; Lautso, P. Geothermal Heat Pump Plant Performance in a Nearly Zero-energy Building. In Proceedings of the Energy Procedia; 2016.
45. Fadejev, J.; Simson, R.; Kurnitski, J.; Kesti, J. Heat Recovery from Exhaust Air as a Thermal Storage Energy Source for Geothermal Energy Piles. In Proceedings of the Energy Procedia; 2016.
46. Hu, B.; Luo, Z. Life-cycle probabilistic geotechnical model for energy piles. *Renew. Energy* **2020**, doi:10.1016/j.renene.2019.09.022.
47. Zalba, B.; Marín, J. M.; Cabeza, L. F.; Mehling, H. Review on thermal energy storage with phase change: Materials, heat transfer analysis and applications. *Appl. Therm. Eng.* 2003.
48. Telkes, M. Thermal storage for solar heating and cooling. In Proceedings of the Workshop on Solar Energy Storage Subsystems for the Heating and Cooling of Buildings; Lembit U., L., James Taylor, B., Fulvio Anthony, I., Eds.; The Society: Charlottesville, 1975.
49. Barkmann, H.; Wessling, J. Use of buildings structural components for thermal storage. In Proceedings of the Workshop on Solar Energy Storage Subsystems for the Heating and Cooling of Buildings; Lembit U. L., James Taylor, B., Fulvio Anthony, I., Eds.; The Society: Charlottesville, 1975.

50. Abhat, A. Low temperature latent heat thermal energy storage: Heat storage materials. *Sol. Energy* **1983**, doi:10.1016/0038-092X(83)90186-X.
51. Zeinelabdein, R.; Omer, S.; Gan, G. Critical review of latent heat storage systems for free cooling in buildings. *Renew. Sustain. Energy Rev.* **2018**, *82*, 2843–2868, doi:10.1016/j.rser.2017.10.046.
52. Cárdenas, B.; León, N. High temperature latent heat thermal energy storage: Phase change materials, design considerations and performance enhancement techniques. *Renew. Sustain. Energy Rev.* 2013.
53. Lane GA. *Solar Heat Storage: Latent Heat Materials Volume 1: Background and Scientific Principles*; CRC Press: London, New York, 1983; ISBN 9781315897653.
54. Dieckmann, J.H.; Heinrich, H. *Betonwerk und Fertigteil-Technik/Concrete Plant and Precast Technology*. 2008, pp. 10–17.
55. Whiffen, T.R.; Riffat, S.B. A review of PCM technology for thermal energy storage in the built environment: Part I. *Int. J. Low-Carbon Technol.* **2013**, doi:10.1093/ijlct/cts021.
56. Koschenz, M.; Lehmann, B. Development of a thermally activated ceiling panel with PCM for application in lightweight and retrofitted buildings. *Energy Build.* **2004**, doi:10.1016/j.enbuild.2004.01.029.
57. Frusteri, F.; Leonardi, V.; Vasta, S.; Restuccia, G. Thermal conductivity measurement of a PCM based storage system containing carbon fibers. *Appl. Therm. Eng.* **2005**, doi:10.1016/j.applthermaleng.2004.10.007.
58. Sari, A.; Karaipekli, A. Thermal conductivity and latent heat thermal energy storage characteristics of paraffin/expanded graphite composite as phase change material. *Appl. Therm. Eng.* **2007**, doi:10.1016/j.applthermaleng.2006.11.004.
59. Cabeza, L. F.; Castell, A.; Barreneche, C.; De Gracia, A.; Fernández, A. I. Materials used as PCM in thermal energy storage in buildings: A review. *Renew. Sustain. Energy Rev.* 2011.
60. Baetens, R.; Jelle, B. P.; Gustavsen, A. Phase change materials for building applications: A state-of-the-art review. *Energy Build.* 2010.
61. Hunger, M.; Entrop, A. G.; Mandilaras, I.; Brouwers, H. J. H.; Founti, M. The behavior of self-compacting concrete containing micro-encapsulated Phase Change Materials. *Cem. Concr. Compos.* **2009**, doi:10.1016/j.cemconcomp.2009.08.002.
62. Voelker, C.; Kornadt, O.; Ostry, M. Temperature reduction due to the application of phase change materials. *Energy Build.* **2008**, doi:10.1016/j.enbuild.2007.07.008.
63. Arce, P.; Castellón, C.; Castell, A.; Cabeza, L. F. Use of microencapsulated PCM in buildings and the effect of adding awnings. *Energy Build.* **2012**, *44*, 88–93, doi:10.1016/j.enbuild.2011.10.028.
64. Evola, G.; Marletta, L.; Sicurella, F. A methodology for investigating the effectiveness of PCM wallboards for summer thermal comfort in buildings. *Build. Environ.* **2013**, *59*, 517–527, doi:10.1016/j.buildenv.2012.09.021.

65. Barzin, R.; Chen, J. J. J.; Young, B. R.; Farid, M. M. Application of PCM underfloor heating in combination with PCM wallboards for space heating using price based control system. *Appl. Energy* **2015**, doi:10.1016/j.apenergy.2015.03.027.
66. Kuznik, F.; Virgone, J.; Noel, J. Optimization of a phase change material wallboard for building use. *Appl. Therm. Eng.* **2008**, doi:10.1016/j.applthermaleng.2007.10.012.
67. Heim, D.; Clarke, J. A. Numerical modelling and thermal simulation of PCM-gypsum composites with ESP-r. In Proceedings of the Energy and Buildings; 2004.
68. Zhang, Y.; Lin, K.; Jiang, Y.; Zhou, G. Thermal storage and nonlinear heat-transfer characteristics of PCM wallboard. *Energy Build.* **2008**, doi:10.1016/j.enbuild.2008.03.005.
69. Stovall, T. K.; Tomlinson, J. J. What are the potential benefits of including latent storage in common wallboard? *J. Sol. Energy Eng. Trans. ASME* **1995**, doi:10.1115/1.2847868.
70. Carbonari, A.; De Grassi, M.; Di Perna, C.; Principi, P. Numerical and experimental analyses of PCM containing sandwich panels for prefabricated walls. *Energy Build.* **2006**, doi:10.1016/j.enbuild.2005.08.007.
71. Evers, A. C.; Medina, M. A.; Fang, Y. Evaluation of the thermal performance of frame walls enhanced with paraffin and hydrated salt phase change materials using a dynamic wall simulator. *Build. Environ.* **2010**, doi:10.1016/j.buildenv.2010.02.002.
72. Halford, C. K.; Boehm, R. F. Modeling of phase change material peak load shifting. *Energy Build.* **2007**, doi:10.1016/j.enbuild.2006.07.005.
73. Alawadhi, E. M. Thermal analysis of a building brick containing phase change material. *Energy Build.* **2008**, doi:10.1016/j.enbuild.2007.03.001.
74. Alawadhi, E. M.; Alqallaf, H. J. Building roof with conical holes containing PCM to reduce the cooling load: Numerical study. *Energy Convers. Manag.* **2011**, doi:10.1016/j.enconman.2011.04.004.
75. Osterman, E.; Hagel, K.; Rathgeber, C.; Butala, V.; Stritih, U. Parametrical analysis of latent heat and cold storage for heating and cooling of rooms. *Appl. Therm. Eng.* **2015**, *84*, 138–149, doi:10.1016/j.applthermaleng.2015.02.081.
76. Darzi, A. A. R.; Moosania, S. M.; Tan, F. L.; Farhadi, M. Numerical investigation of free-cooling system using plate type PCM storage. *Int. Commun. Heat Mass Transf.* **2013**, *48*, 155–163, doi:10.1016/j.icheatmasstransfer.2013.08.025.
77. Borcuch, M.; Musiał, M.; Sztekler, K.; Kalawa, W.; Gumuła, S.; Stefański, S. The influence of flow modification on air and PCM temperatures in an accumulative heat exchanger. In Proceedings of the EPJ Web of Conferences; 2018; Vol. 180.
78. Jaworski, M.; Łapka, P.; Furmański, P. Numerical modelling and experimental studies of thermal behaviour of building integrated thermal energy storage unit in a form of a ceiling panel. *Appl. Energy* **2014**, doi:10.1016/j.apenergy.2013.07.068.
79. Jaworski, M. Thermal performance of building element containing phase change material (PCM) integrated with ventilation system - An experimental study. *Appl. Therm. Eng.* **2014**, doi:10.1016/j.applthermaleng.2014.05.093.

80. Borderon, J.; Virgone, J.; Cantin, R. Modeling and simulation of a phase change material system for improving summer comfort in domestic residence. *Appl. Energy* **2015**, *140*, 288–296, doi:10.1016/j.apenergy.2014.11.062.
81. Weinläder, H.; Klinker, F.; Yasin, M. PCM cooling ceilings in the Energy Efficiency Center - Passive cooling potential of two different system designs. *Energy Build.* **2016**, *119*, 93–100, doi:10.1016/j.enbuild.2016.03.031.
82. Ručevskis, S.; Akishin, P.; Korjakins, A. Parametric analysis and design optimisation of PCM thermal energy storage system for space cooling of buildings. *Energy Build.* **2020**, doi:10.1016/j.enbuild.2020.110288.
83. Rucevskis, S.; Akishin, P.; Korjakins, A. Performance Evaluation of an Active PCM Thermal Energy Storage System for Space Cooling in Residential Buildings. *Environ. Clim. Technol.* **2019**, doi:10.2478/rtuect-2019-0056.
84. Rucevskis, S.; Akishin, P.; Korjakins, A. Numerical Study of Application of PCM for a Passive Thermal Energy Storage System for Space Cooling in Residential Buildings. In Proceedings of the IOP Conference Series: Materials Science and Engineering; 2019.
85. Goodfellow, H.; Tahti, E. *Industrial Ventilation Design Guidebook*; Academic Press: Orlando, 2001; ISBN 0-12-289676-9.
86. ASHRAE *ASHRAE Fundamentals*; 2017;
87. Stoecker, W. F.; Jones, J.. *Refrigeration and Air Conditioning*; McGraw-Hill: Auckland, 1982;
88. The Information Philosopher Available online: https://www.informationphilosopher.com/solutions/scientists/planck/.
89. Travesi, J.; Maxwell, G.; Klaassen, C.; Holtz, M. Empirical validation of Iowa energy resource station building energy analysis simulation models. **2001**.
90. Sahlin, P.; Grozman, P. IDA Simulation Environment a tool for Modelica based end-user application deployment. *Proc. 3rd Int. Model. Conf. Linkoping, Novemb. 3-4 2003* **2003**, 105–114.
91. Rubitherm GmbH Technical data sheet for RT22HC 2018, 1.
92. European Committee for Standartization EN 15377-1:2008 Heating systems in buildings. Design of embedded water based surface heating and cooling systems. Determination of the design heating and cooling capacity 2008.
93. Nageler, P.; Schweiger, G.; Pichler, M.; Brandl, D.; Mach, T.; Heimrath, R.; Schranzhofer, H.; Hochenauer, C. Validation of dynamic building energy simulation tools based on a real test-box with thermally activated building systems (TABS). *Energy Build.* **2018**, *168*, 42–55, doi:https://doi.org/10.1016/j.enbuild.2018.03.025.
94. Cornaro, C.; Pierro, M.; Roncarati, D.; Puggioni, V. Validation of a PCM simulation tool in IDA ICE dynamic building simulation software using experimental data from solar test boxes. In Proceedings of the Building Simulation Applications; 2017; Vol. 2017-Febru, pp. 159–166.